

Wright State University

CORE Scholar

Special Session 5: Carbon and Oxide Based
Nanostructured Materials (2012)

Special Session 5

6-2012

Properties of SbSI@CNTs and SbSI Nanowires

Marian Nowak

Krzysztof Koziol

Gregory Kozlowski

Wright State University - Main Campus, gregory.kozlowski@wright.edu

Krystian Mistewicz

Marcin Jesionek

Follow this and additional works at: https://corescholar.libraries.wright.edu/ss5_2012

 Part of the [Physics Commons](#)

Repository Citation

Nowak, M., Koziol, K., Kozlowski, G., Mistewicz, K., & Jesionek, M. (2012). Properties of SbSI@CNTs and SbSI Nanowires. .

https://corescholar.libraries.wright.edu/ss5_2012/4

This Presentation is brought to you for free and open access by the Special Session 5 at CORE Scholar. It has been accepted for inclusion in Special Session 5: Carbon and Oxide Based Nanostructured Materials (2012) by an authorized administrator of CORE Scholar. For more information, please contact library-corescholar@wright.edu.

Properties of SbSI@CNTs and SbSI nanowires

M. Nowak¹, K. Koziol², G. Kozlowski³,
K. Mistewicz¹, M. Jesionek¹

¹ Institute of Physics, Silesian University of Technology, Katowice, Poland.

² Department of Materials Science, University of Cambridge, Cambridge, UK.

³ Department of Physics, Wright State University, Dayton, Ohio, USA.

Subjects presented¹ at DSL-2011:

- sonochemical preparation of **antimony sulfoiodide** (SbSI)-type nanowires,
- sonochemical filling of carbon nanotubes with SbSI (SbSI @ CNTs),
- ultrasonic welding of CNTs to metal electrodes.

[1] M. Nowak, K. Koziol, G. Kozlowski, J. Berdowski, J. Kasperczyk, I. Kityk, K. Mistewicz, M. Jesionek, **Ultrasonics and Carbon Nanotubes** , Special Session: Carbon and Oxide Based Nanostructured Materials at the 7th Internat. Conf. DSL-2011, Algarve, Portugal. ²

Properties of SbSI

- **semiconductor** ($E_{g/f} = 1.83(3) \text{ eV}$)

Properties of SbSI

- semiconductor ($E_{glf} = 1.83(3) \text{ eV}$)
- **ferroelectric** ($T_c = 292(1) \text{ K}$)

Properties of SbSI

- semiconductor ($E_{g/f} = 1.83(3) \text{ eV}$)
- ferroelectric ($T_c = 292(1) \text{ K}$)
- **high spontaneous polarization** ($P_s = 0.30 \text{ C/m}^2$)

Properties of SbSI

- semiconductor ($E_{glf} = 1.83(3) \text{ eV}$)
- ferroelectric ($T_c = 292(1) \text{ K}$)
- high spontaneous polarization ($P_s = 0.30 \text{ C/m}^2$)
- **low coercive field** ($E_c = 10^4 \text{ V/m}$ ($T = 0^\circ\text{C}$, 50 Hz))

Properties of SbSI

- semiconductor ($E_{g/f} = 1.83(3) \text{ eV}$)
- ferroelectric ($T_c = 292(1) \text{ K}$)
- high spontaneous polarization ($P_s = 0.30 \text{ C/m}^2$)
- low coercive field $E_c = 10^4 \text{ V/m}$ ($T = 0^\circ\text{C}$, 50 Hz)
- **high electromechanical coupling** ($k_{33} = 0.9$)

Properties of SbSI

- **high piezoelectric modulus** ($d_{333}=7(2 \cdot 10^{-9} \text{ m/V})$)

Properties of SbSI

- high piezoelectric modulus ($d_{333}=7(2 \cdot 10^{-9} \text{ m/V})$)
- **strong electrostriction** ($Q_{3333}=1.5 \cdot 10^{-13} \text{ m}^2/\text{V}^2$)

Properties of SbSI

- high piezoelectric modulus ($d_{333}=7(2 \cdot 10^{-9} \text{ m/V})$)
- strong electrostriction ($Q_{3333}=1.5 \cdot 10^{-13} \text{ m}^2/\text{V}^2$)
- very high pyro-optical coefficient along c axis
($1.5 \cdot 10^{-3} \text{ K}^{-1}$)

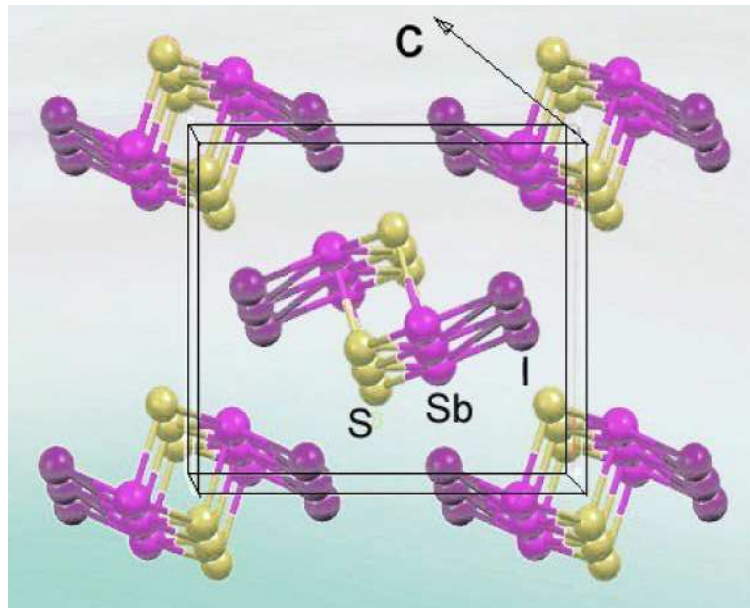
Properties of SbSI

- high piezoelectric modulus ($d_{333}=7(2 \cdot 10^{-9} \text{ m/V})$)
- strong electrostriction ($Q_{3333}=1.5 \cdot 10^{-13} \text{ m}^2/\text{V}^2$)
- very high pyro-optical coefficient along c axis
($1.5 \cdot 10^{-3} \text{ K}^{-1}$)
- **pyroelectric** (60 mC/(m²K))

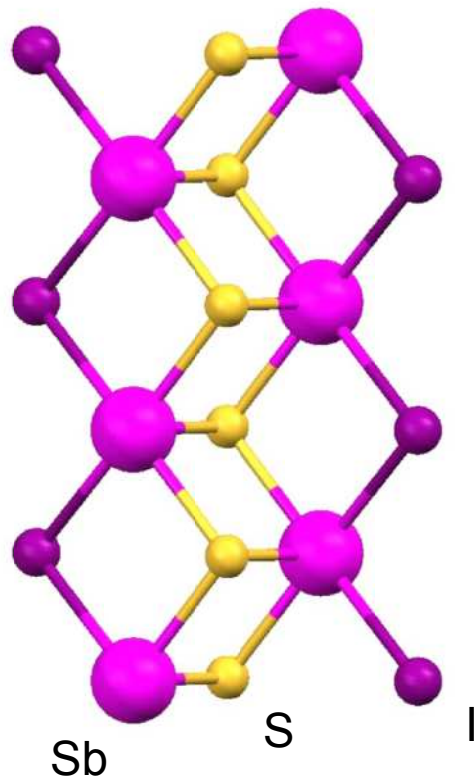
Properties of SbSI

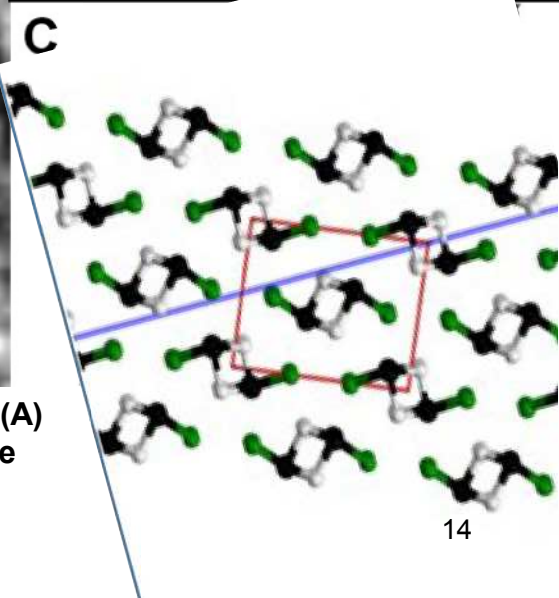
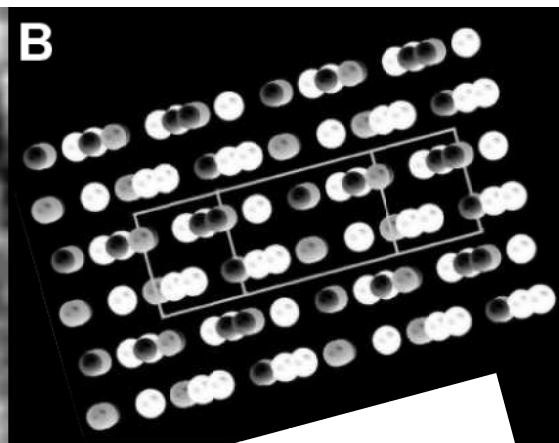
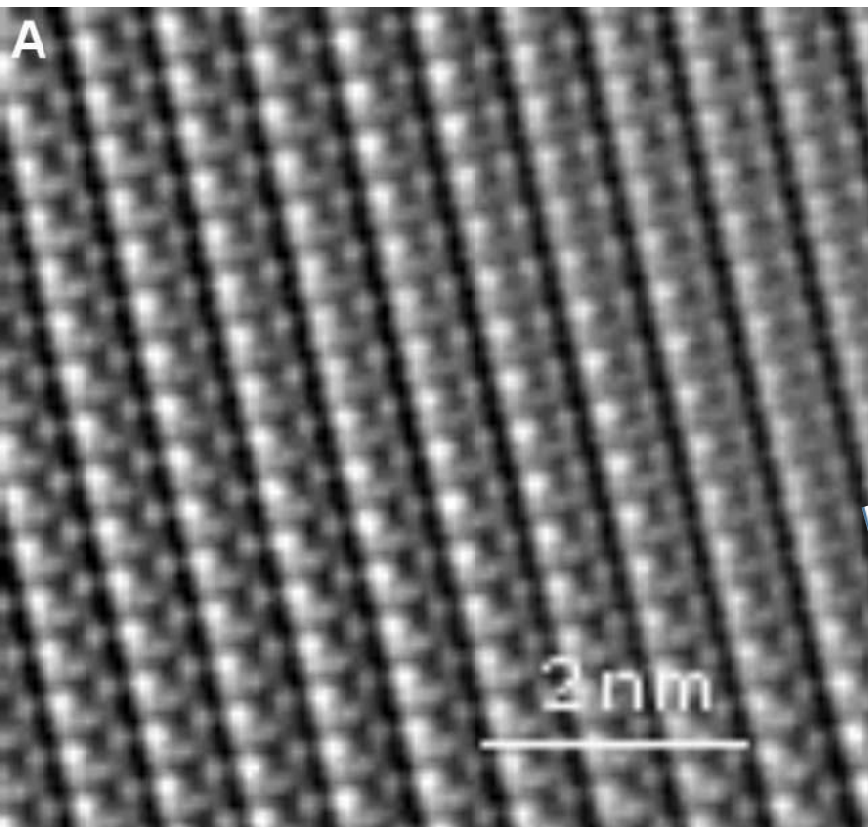
- high piezoelectric modulus ($d_{333}=7(2 \cdot 10^{-9} \text{ m/V})$)
- strong electrostriction ($Q_{3333}=1.5 \cdot 10^{-13} \text{ m}^2/\text{V}^2$)
- very high pyro-optical coefficient along c axis
($1.5 \cdot 10^{-3} \text{ K}^{-1}$)
- pyroelectric (60 mC/(m²K))
- strong anisotropy

- strong anisotropy



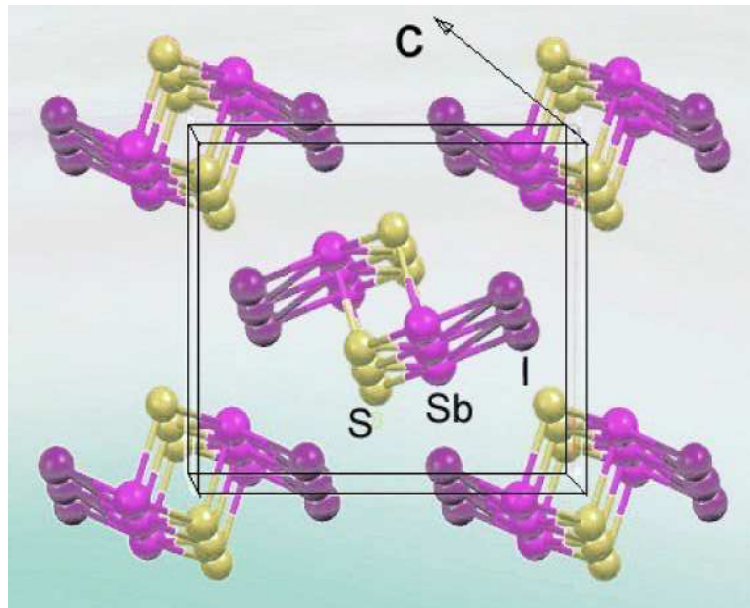
$a = 0.853 \text{ nm}$, $b = 1.017 \text{ nm}$,
 $c = 0.408 \text{ nm}$



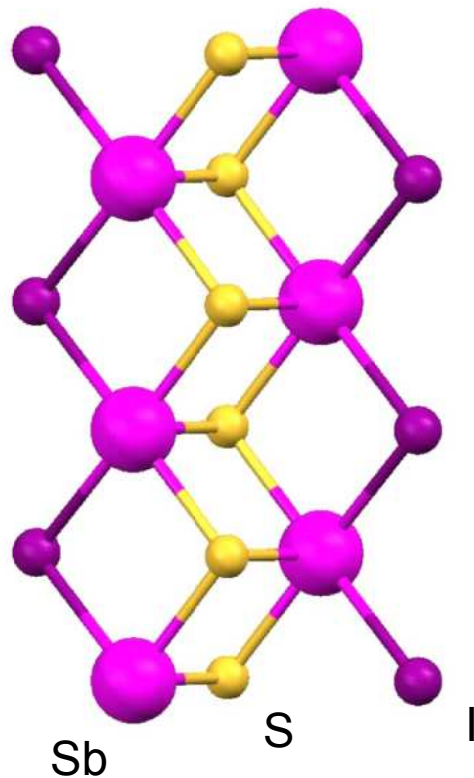


Comparison of filtered HRTEM image of SbSI nanowires (A) with calculated distribution of atoms (B- view comparable with the experiment; C- view along the c axis of the SbSI nanowires; ● Sb, ● S and ● I atoms; line shows the (210) plane; red rectangle presents cell in SbSI crystal).

- strong anisotropy

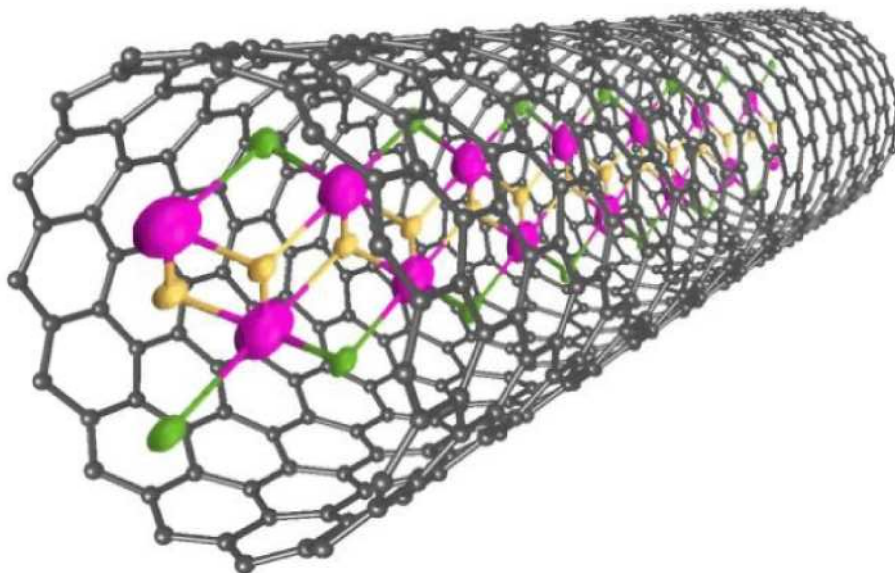


$a = 0.853 \text{ nm}$, $b = 1.017 \text{ nm}$,
 $c = 0.408 \text{ nm}$

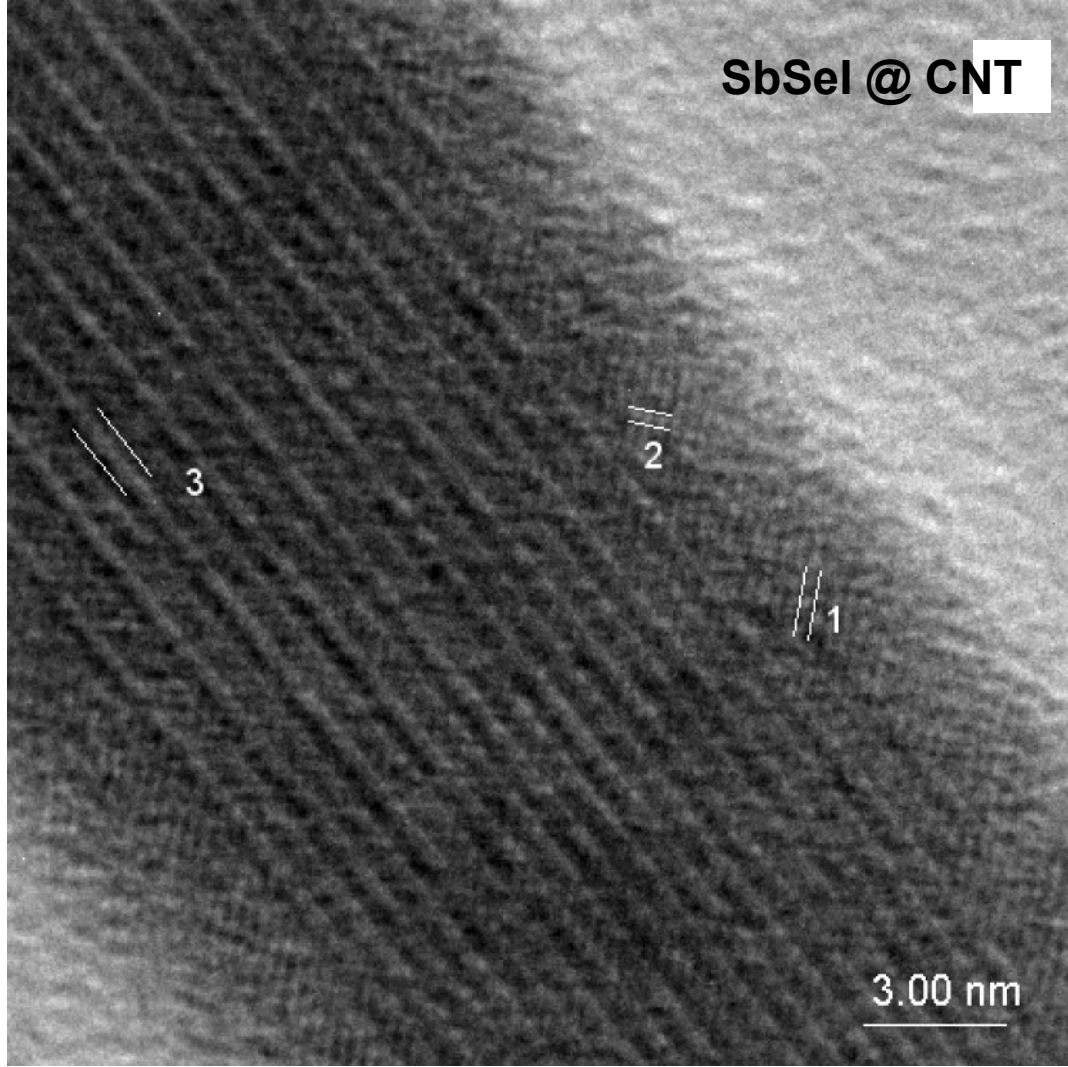


SbSI @ CNTs

SbSeI @ CNTs

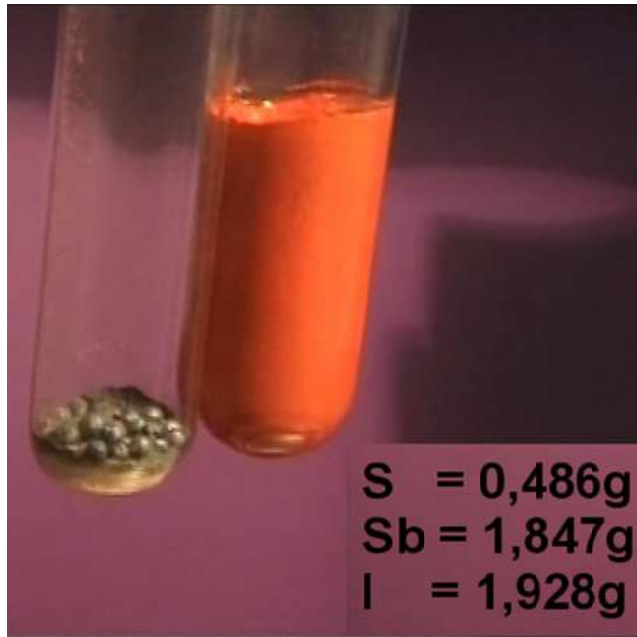
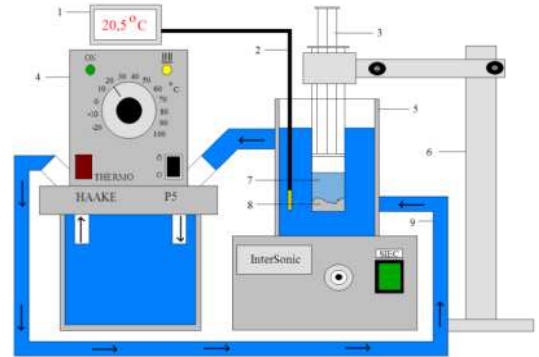


SbSeI @ CNT



The **sonochemical technique** based on **cavitation** is :

- convenient,
- fast,
- efficient technique of nanotechnology.



**Befor and after
sonochemical synthesis
of SbSI in ethanol**

**S = 0,486g
Sb = 1,847g
I = 1,928g**

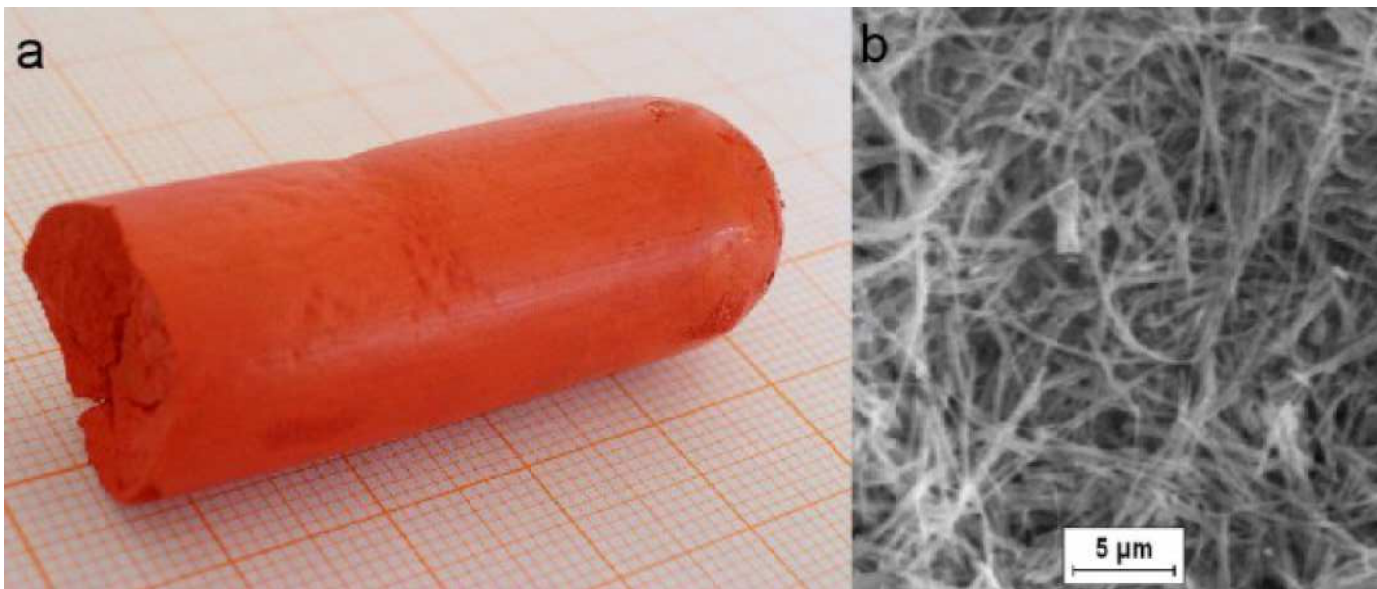
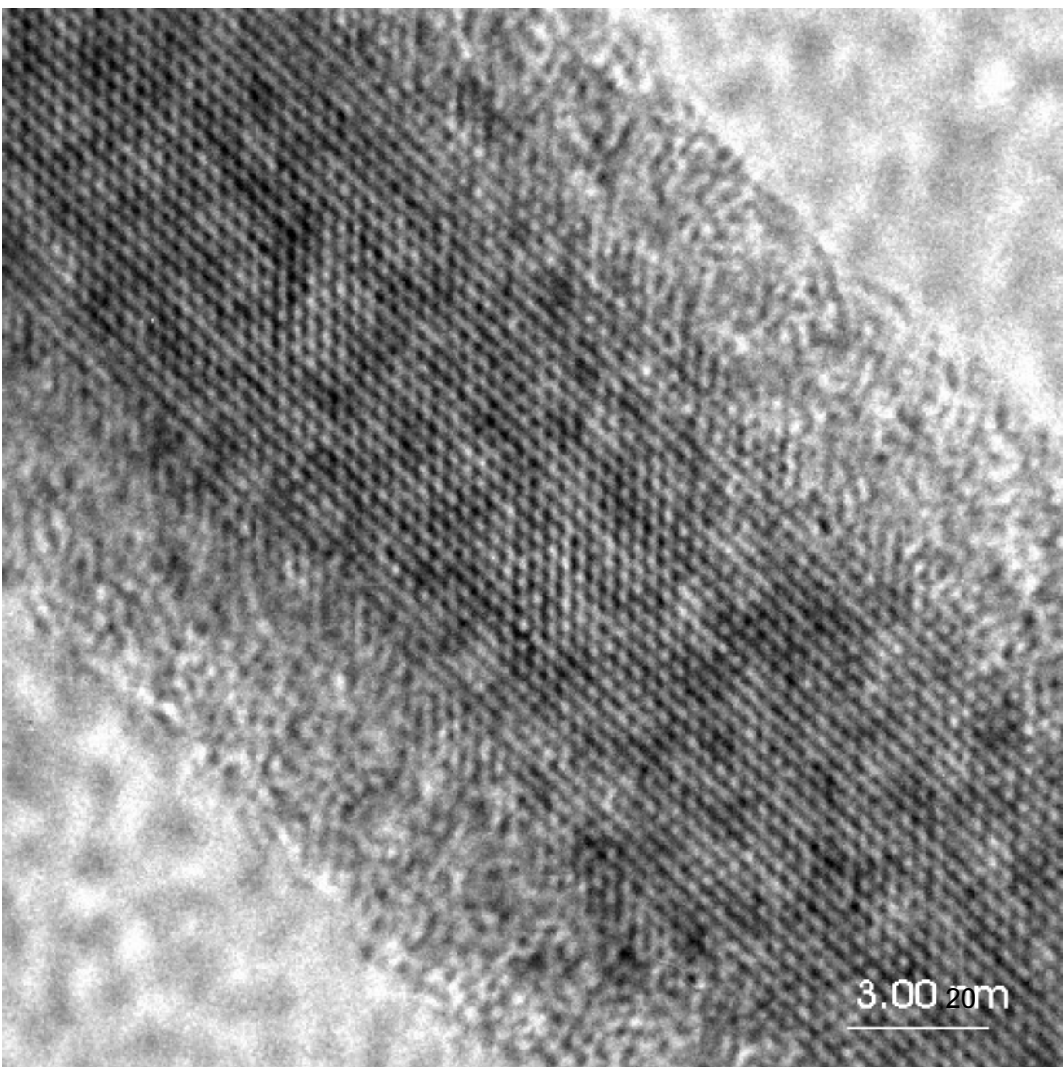


Image (a) and typical SEM micrograph (b) of sonochemically prepared SbSI gel.

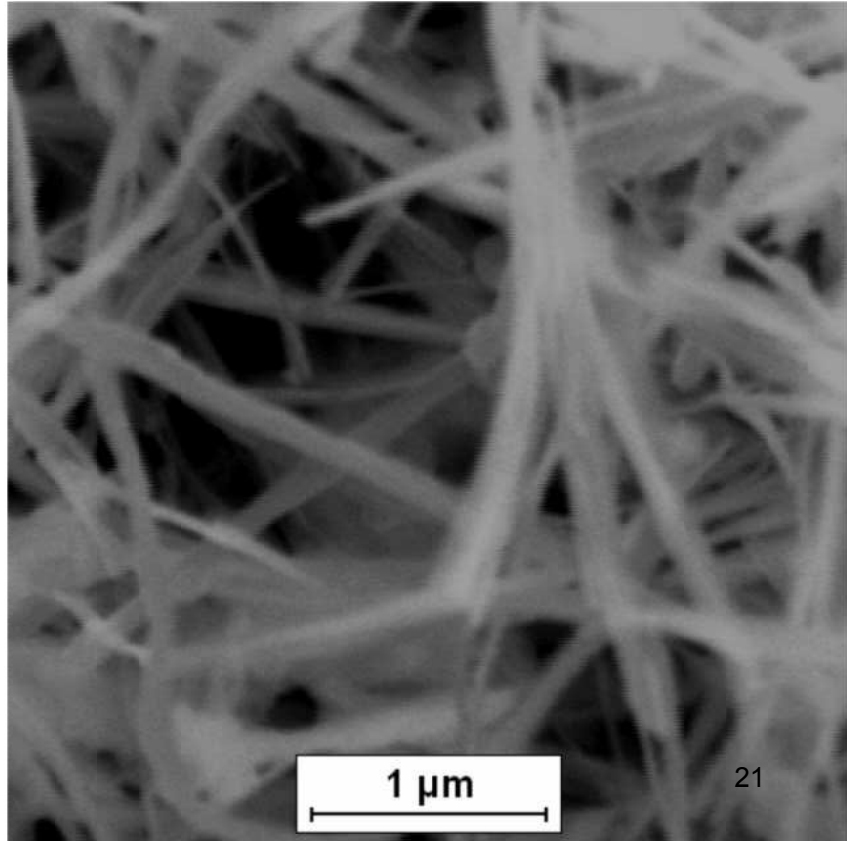
**HRTEM image of
individual
nanowire of SbSI**

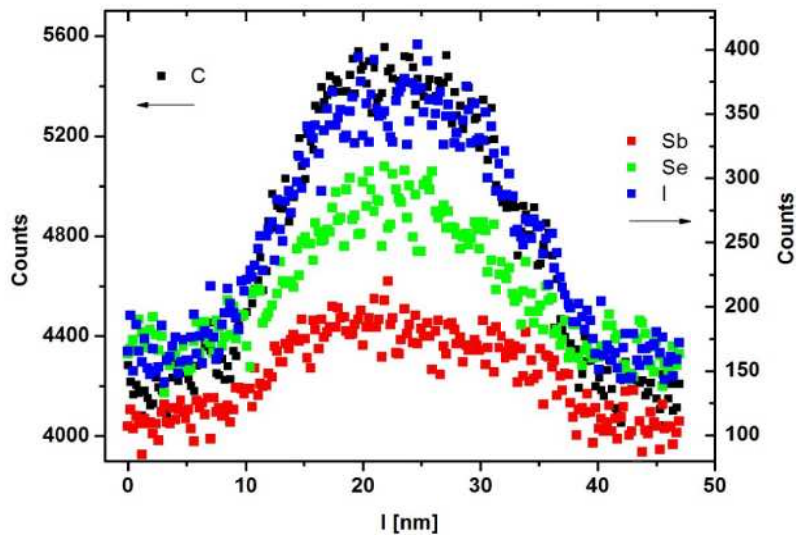
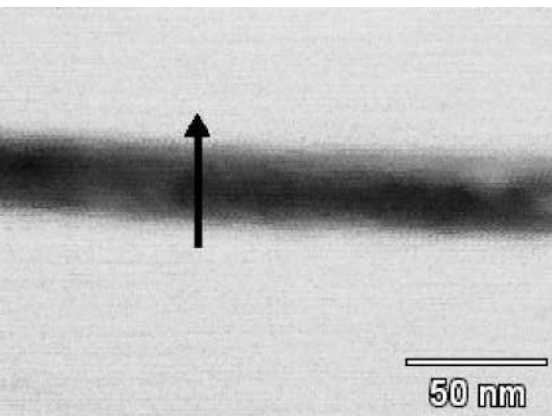




Dried multiwalled CNTs filled with SbSI sonochemically in methanol.

Typical SEM micrograph of dried multiwalled CNTs filled with SbSI sonochemically in methanol.





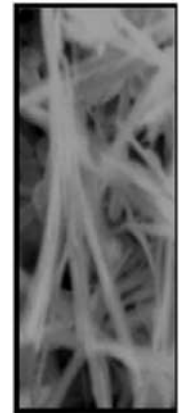
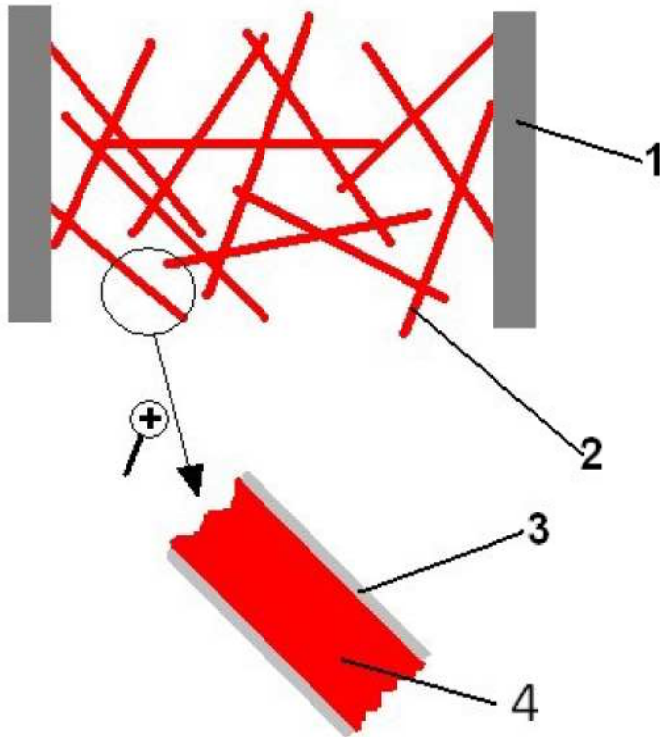
TEM line scan EDS for SbSeI encapsulated in CNT

New subject:

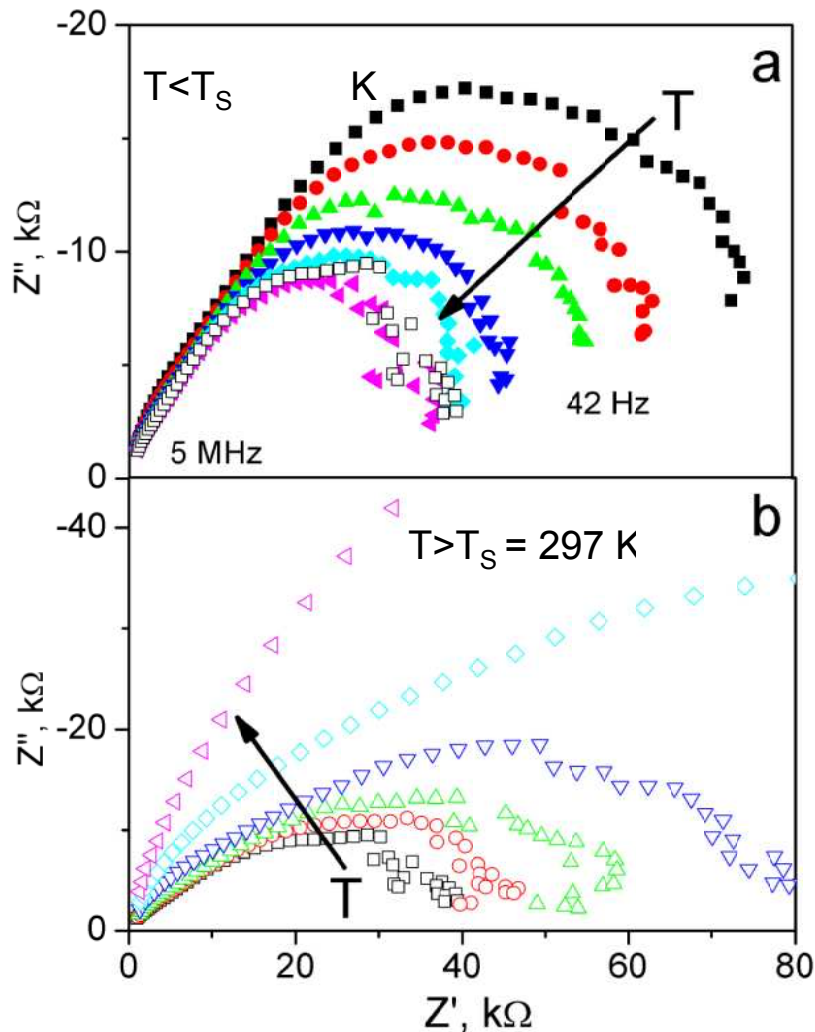
sensing properties

**of SbSI @ CNTs and
SbSI nanowires**

Electrical investigations of no welded SbSI@CNTs or SbSI nanowires



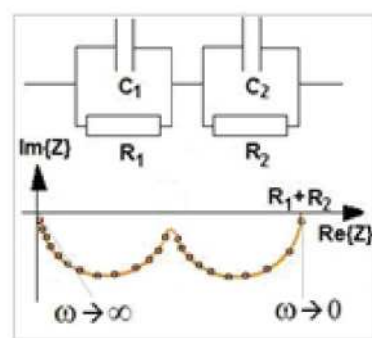
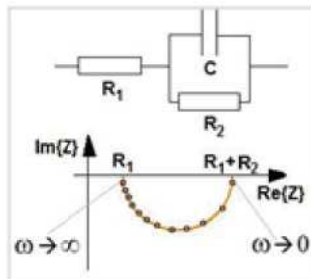
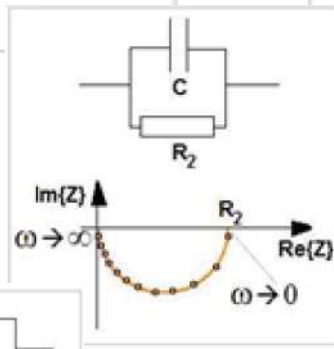
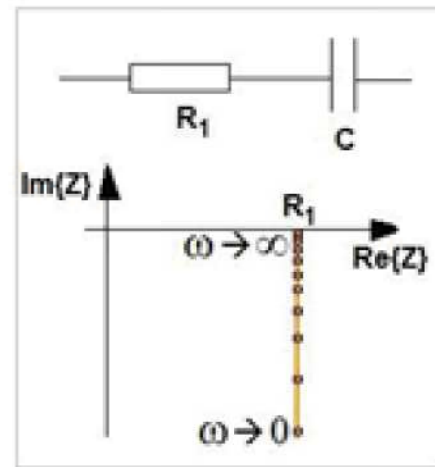
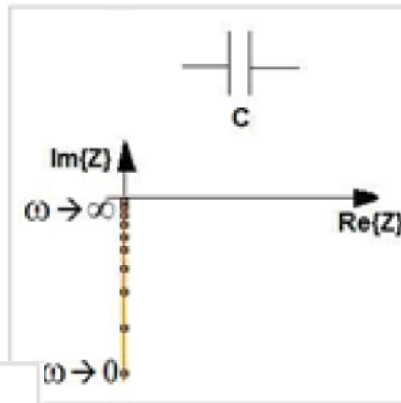
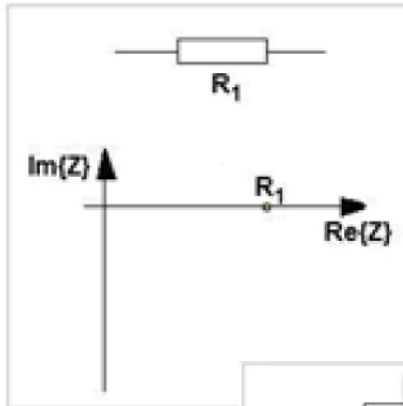
1- electrodes,
2- SbSI@CNTs or SbSI nanowire,
3- CNT or surface layer,
4- SbSI nanowire.

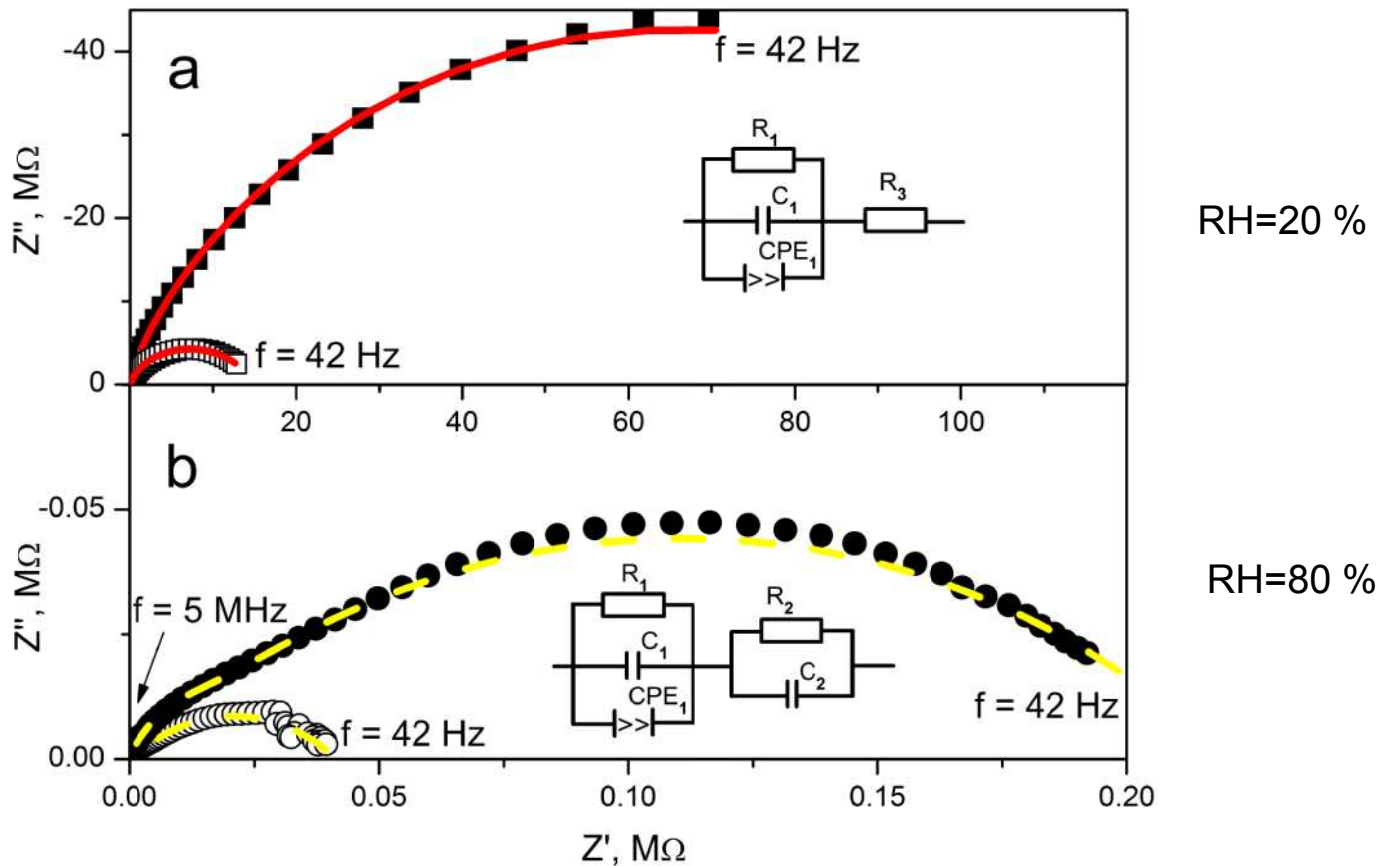


Influence of temperature and humidity on Nyquist plots of SbSI gel

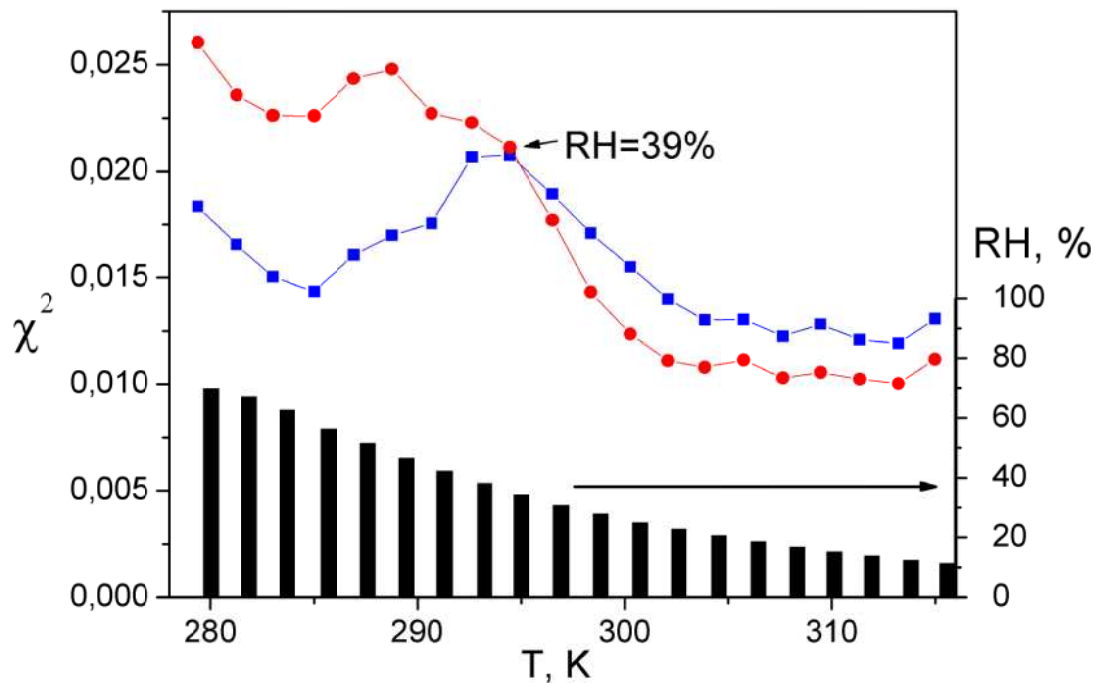
- - $T=289 \text{ K}$, $\text{RH}=87\%$;
 - □ - $T=291 \text{ K}$, $\text{RH}=86\%$;
 - ▲ - $T=293 \text{ K}$, $\text{RH}=85\%$;
 - ▼ - $T=295 \text{ K}$, $\text{RH}=84\%$;
 - ◆ - $T=297 \text{ K}$, $\text{RH}=84\%$;
 - ◆ - $T=299 \text{ K}$, $\text{RH}=83\%$;
 - - $T=300 \text{ K}$, $\text{RH}=80\%$;
 - - $T=302 \text{ K}$, $\text{RH}=57\%$;
 - △ - $T=304 \text{ K}$, $\text{RH}=45\%$;
 - ▽ - $T=306 \text{ K}$, $\text{RH}=41\%$;
 - ◇ - $T=308 \text{ K}$, $\text{RH}=36\%$;
 - ◇ - $T=310 \text{ K}$, $\text{RH}=34\%$;
- $E = 290 \text{ V/m}$, $p = 1 \text{ atm}$).

Impedance spectroscopy



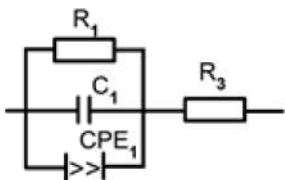


Influence of temperature on Nyquist plot for SbSI gel for constant humidity
 (■ – $T=281 \text{ K}$; □ – $T=304 \text{ K}$; ● – $T=281 \text{ K}$; ○ – $T=300 \text{ K}$).

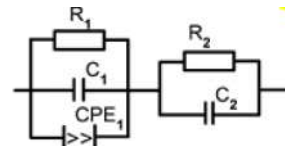


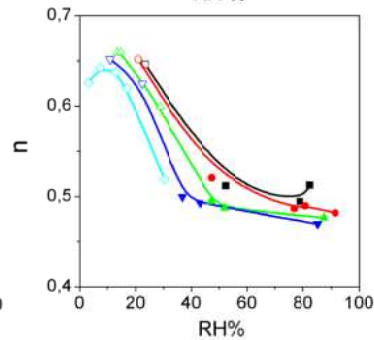
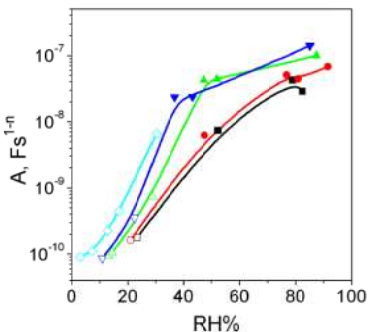
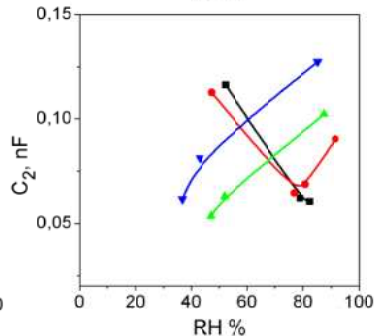
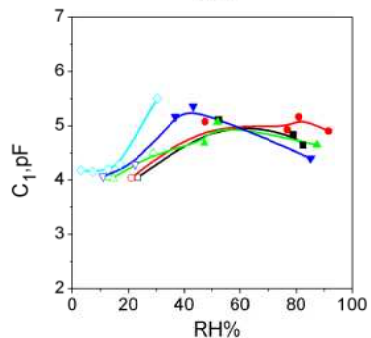
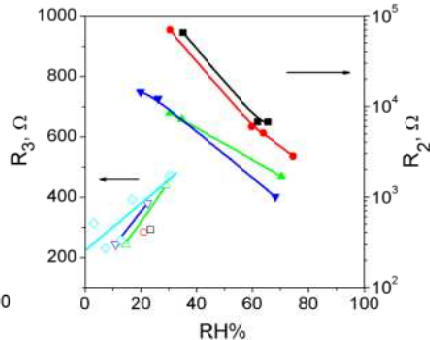
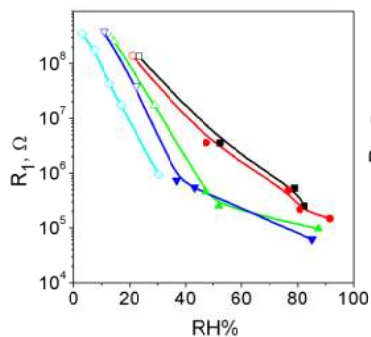
Sum of the least squares obtained when data registered under different ambient conditions of SbSI gel (black bars) were fitted with different models

● for



■ for

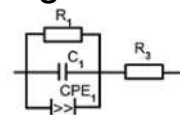




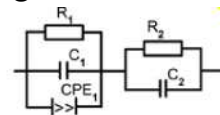
Influence of humidity on resistance and capacitance parameters of equivalent circuits used to interpret Nyquist plots for different temperatures

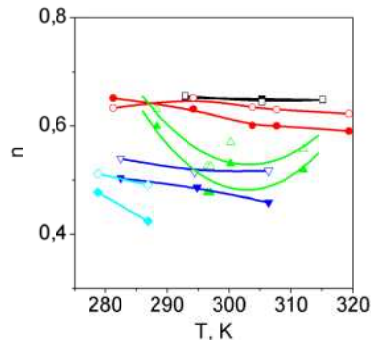
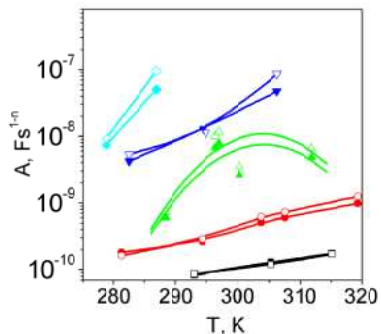
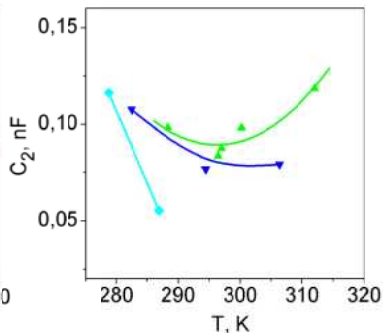
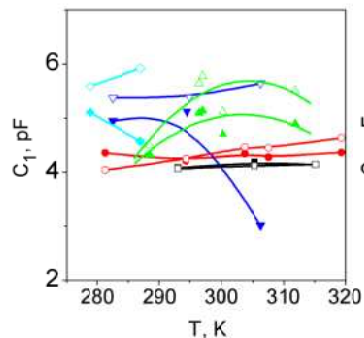
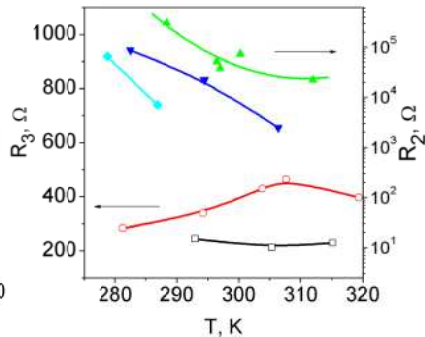
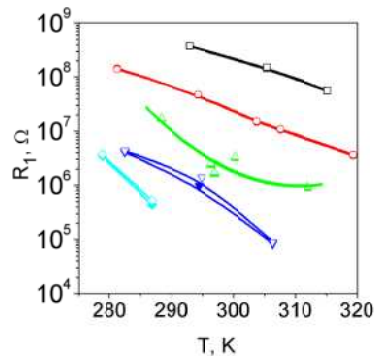
- - RH= 10 %;
- - RH= 20 %;
- ▲ - RH= 30 %;
- ▼ - RH= 40 %;
- ◆ - RH= 55 %)

open signs – model:



full signs – model:

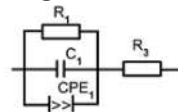




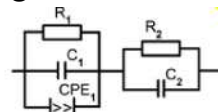
Influence of temperature on resistance and capacitance parameters of equivalent circuits used to interpret Nyquist plots for different humidities

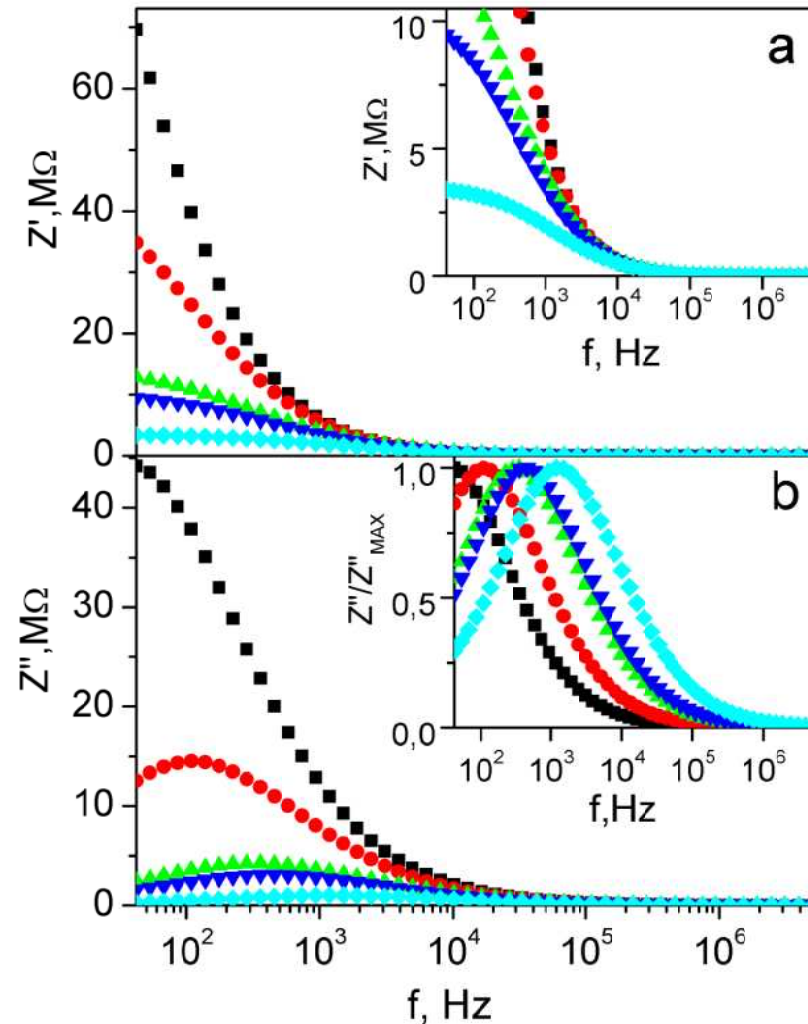
- - RH= 10 %;
- - RH= 20 %;
- ▲ - RH= 30 %;
- ▼ - RH= 40 %;
- ◆ - RH= 55 %)

open signs – model:



full signs – model:

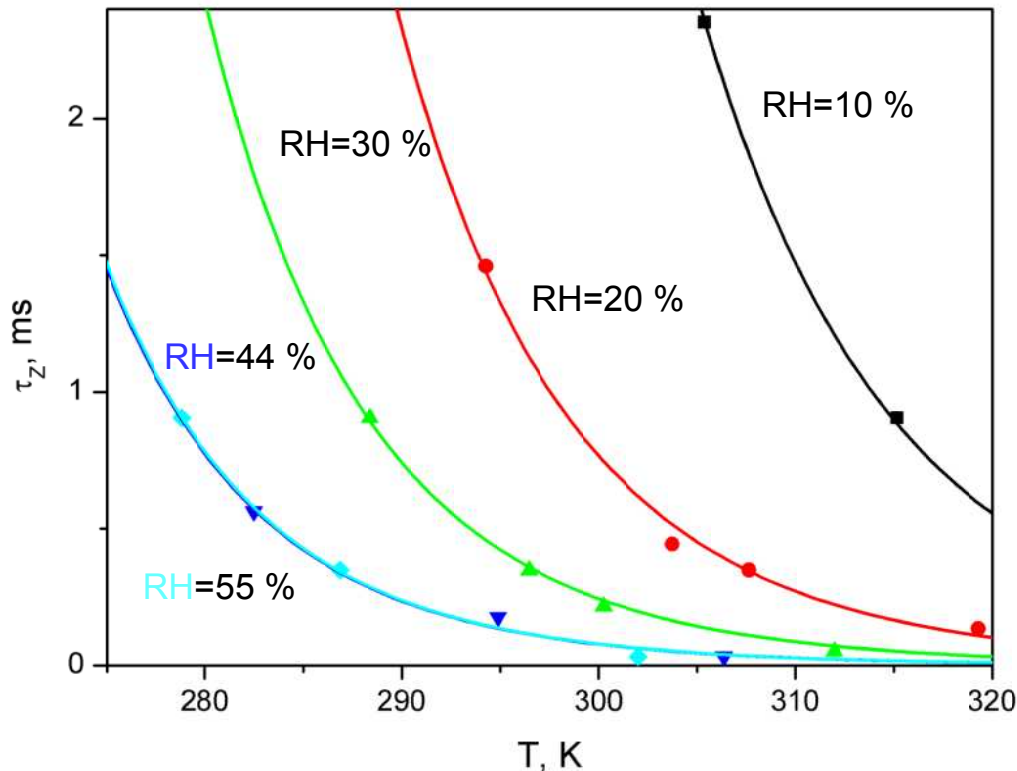




Influence of temperature on frequency response of real (a) and imaginary (b) parts of impedance of SbSI gel for constant humidity:

- - $T=281 \text{ K}$; $\text{RH}=20 \%$
- □ - $T=294 \text{ K}$; $\text{RH}=20 \%$
- ▲ - $T=304 \text{ K}$; $\text{RH}=20 \%$
- ▼ - $T=307 \text{ K}$; $\text{RH}=20 \%$
- ◆ - $T=319 \text{ K}$; $\text{RH}=20 \%$

$$2 \pi f_{\text{MAX}} \tau_Z = 1$$

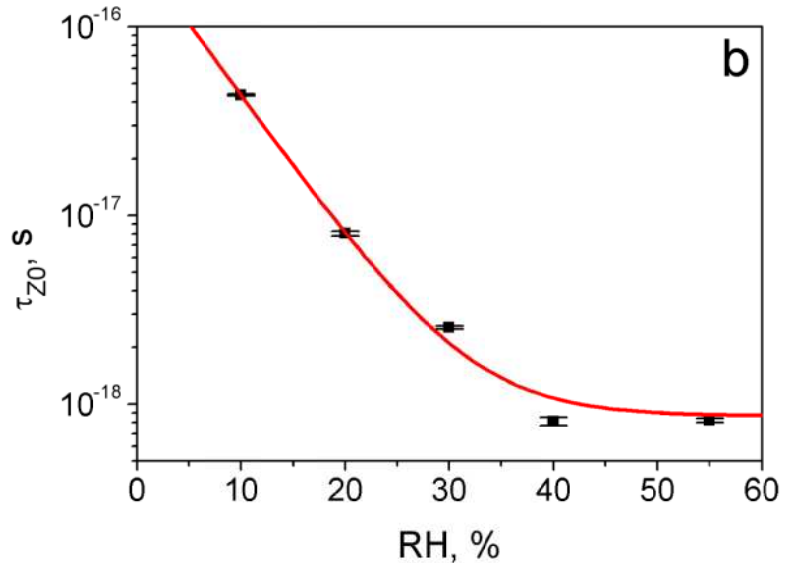


Influence of temperature and humidity on relaxation time of SbSI gel

$$\tau_Z = \tau_{Z0} \exp\left(\frac{E_a}{k_B T}\right)$$

$$E_a = (0.832 \pm 0.067) \text{ eV}_{32}$$

$$\tau_Z = \tau_{Z0} \exp\left(\frac{E_a}{k_B T}\right)$$

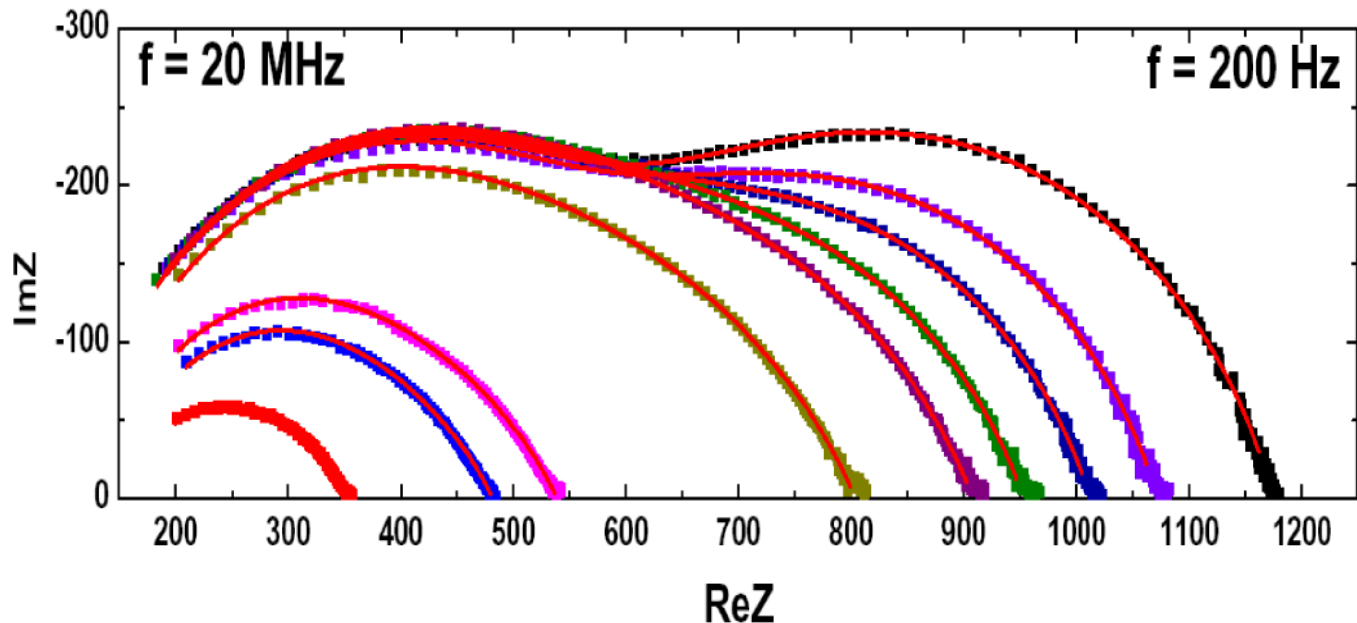


Influence of humidity on pre-exponential factor describing temperature dependence of relaxation time of SbSI gel

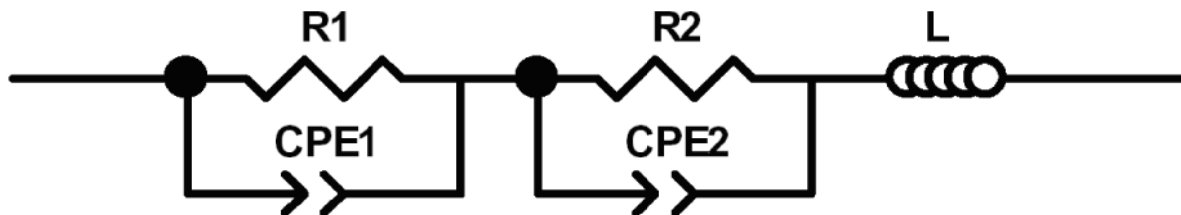
$$\tau_{Z0}(RH) = \tau_{Z0}(RH = 0) \exp\left(\frac{-RH}{B}\right) + \tau_{ZRHmax}$$

$$t_{Z0}(RH=0) = (2.49 \pm 0.15) \cdot 10^{-16} \text{ s}, \quad B = 5.7 \pm 0.2, \quad t_{ZRHmax} = (0.87 \pm 0.15) \cdot 10^{-18} \text{ s}$$

SbSI @ CNTs



Influence of temperature on Nyquist plots for CNTs filled with SbSI (■ – 273 K, ■ – 283 K, ■ – 293 K, ■ – 303 K, ■ – 313 K, ■ – 323 K, ■ – 333 K, ■ – 343 K, ■ – 353 K). Solid curves represent the fitted theoretical dependences calculated for an equivalent circuit.

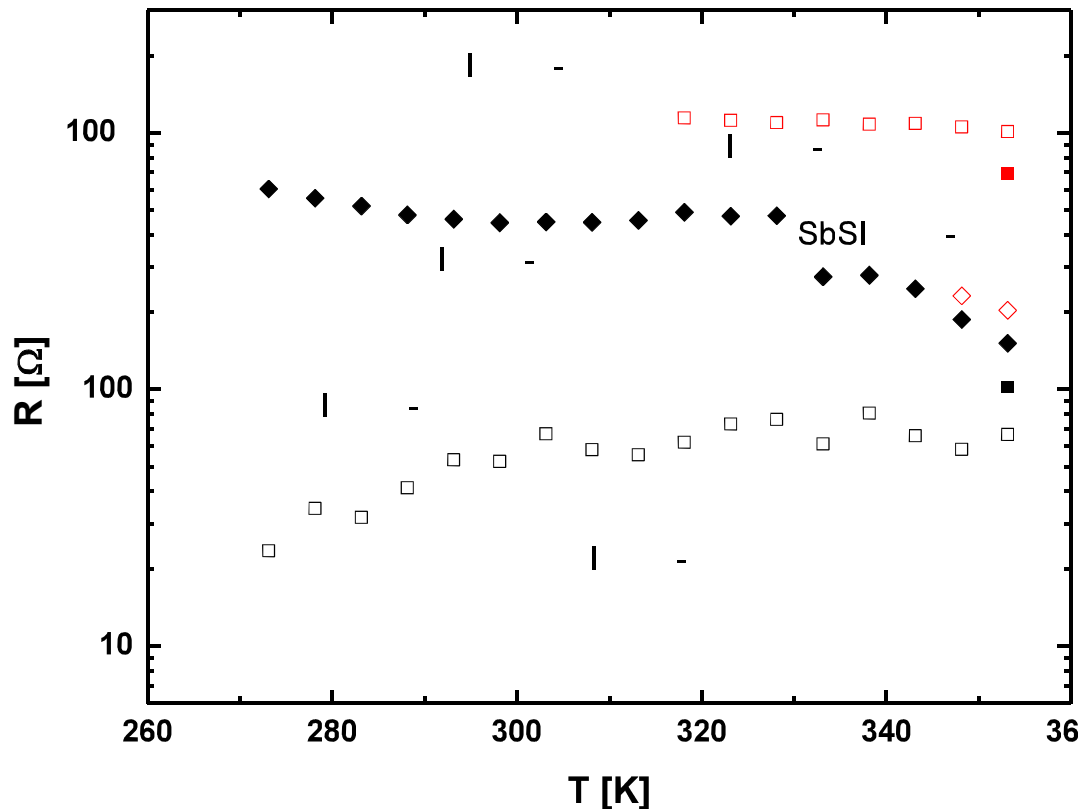


Equivalent circuit describing Nyquist plot of SbSI@CNT sonochemically prepared in methanol

Impedance of  constant phase element (CPE)

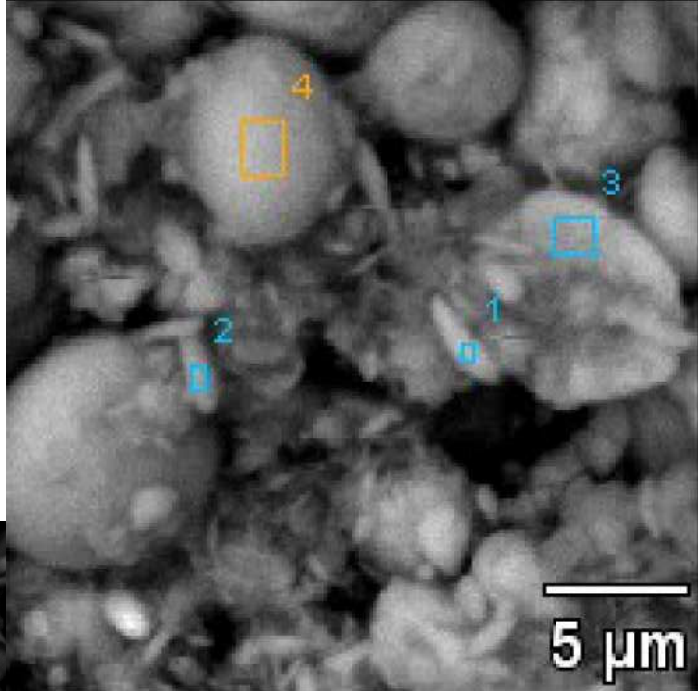
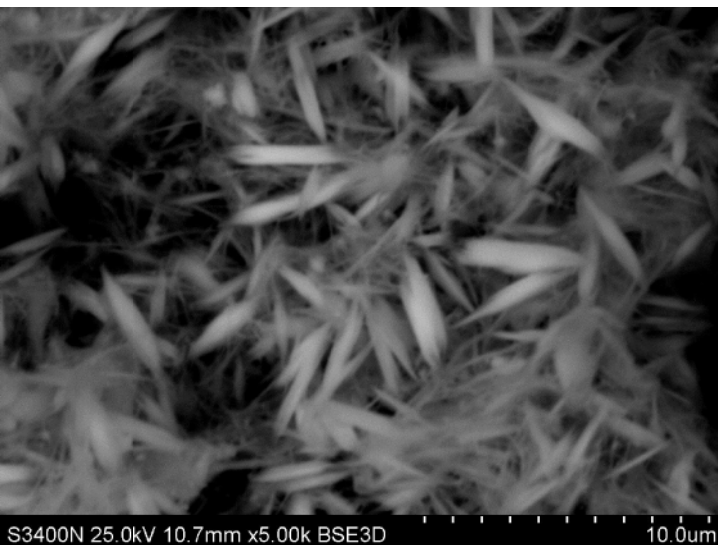
$$Z_{CPE} = \left[A(j\omega)^n \right]^{-1}$$

$n = 1$ for ideal capacitor and $n = 0$ for ideal resistor

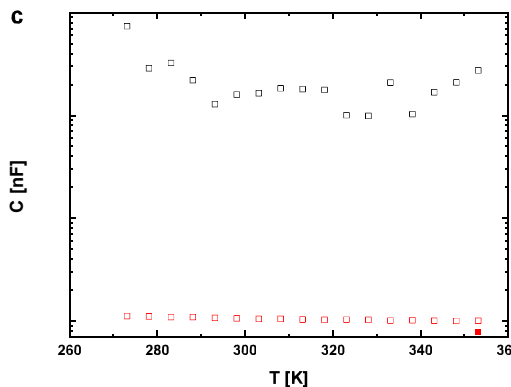
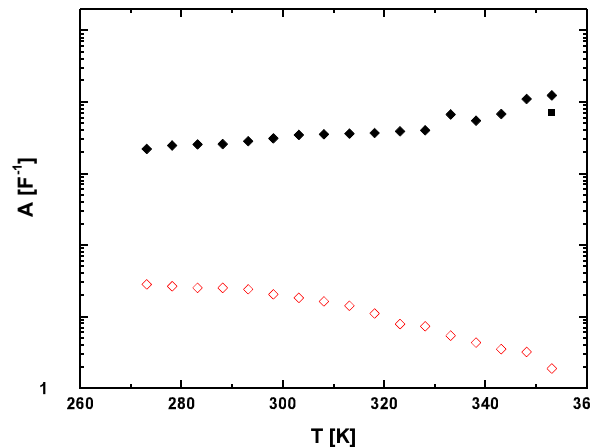
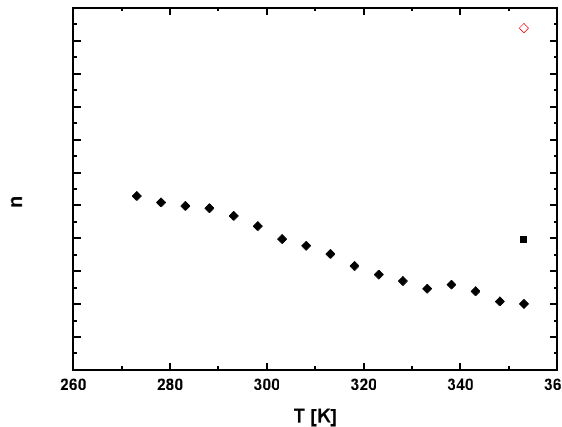


Comparison of the temperature dependences of resistance parameters of equivalent circuits describing Nyquist plots registered in the cases of SbSI@CNT sonochemically prepared in methanol ($\diamond - R_1$, $\blacklozenge - R_2$), and SbSI@CNT ($\color{red}\square - R_1$, $\blacksquare - R_2$) and SbSel@CNT ($\color{red}\diamond - R_1$, $\color{red}\square - R_2$) ultrasonically prepared in ethanol.

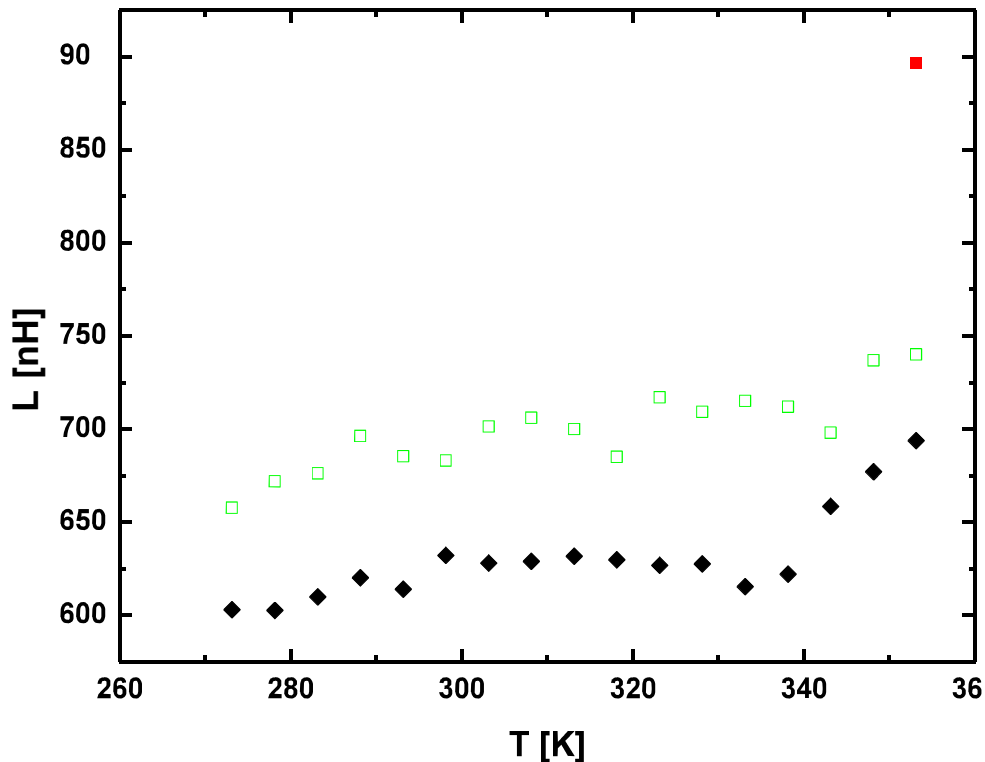
**SbSI after 30 min. of
sonochemical synthesis
in toluene**



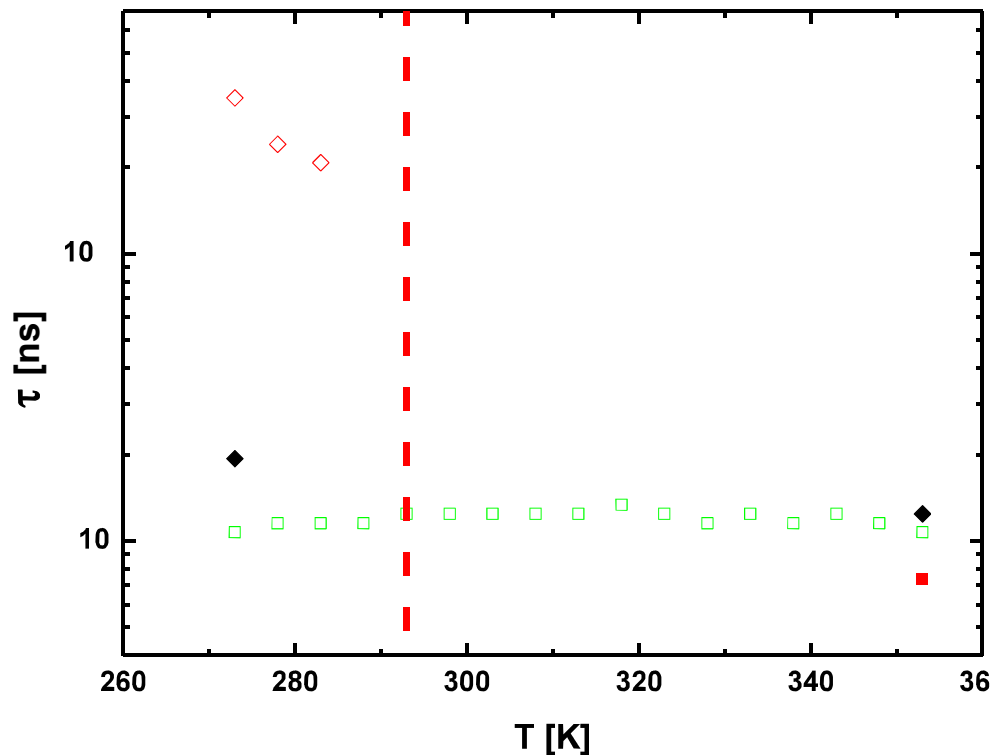
**SbSI after 120 min. of
sonochemical synthesis
in toluene**



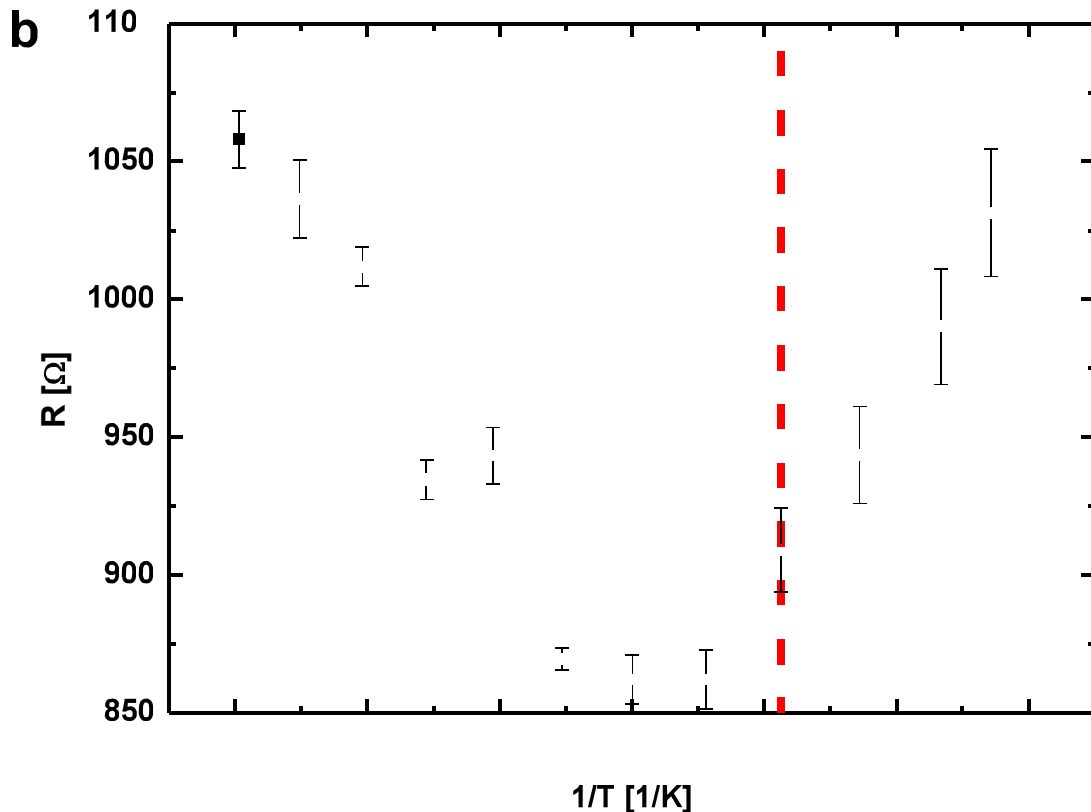
Comparison of capacitance parameters of equivalent circuits describing Nyquist plots of SbSI@CNT sonochemically prepared in methanol (\blacklozenge – n_1 , A_1 ; \redlozenge – n_2 , A_2), and SbSI@CNT (\blacksquare – n , A ; \redsquare – C) and SbSel@CNT (\square – C_{138} , \redsquare – C_2) sonochemically prepared in ethanol.



Comparison of inductance parameters of equivalent circuits describing Nyquist plots of SbSI@CNT sonochemically prepared in methanol (\blacklozenge), and SbSI@CNT (\blacksquare) and SbSeI@CNT (\square) ultrasonically prepared in ethanol³⁹

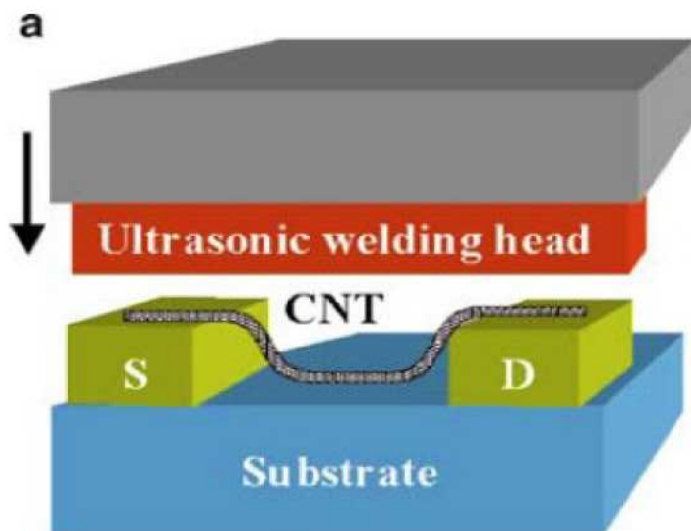


Comparison of the temperature dependences of relaxation time of SbSI@CNT sonochemically prepared in methanol ($\blacklozenge - t_1$, $\redlozenge - t_2$), and SbSI@CNT (\redsquare) and SbSeI@CNT (\greenbox) ultrasonically prepared in ethanol.⁴⁰

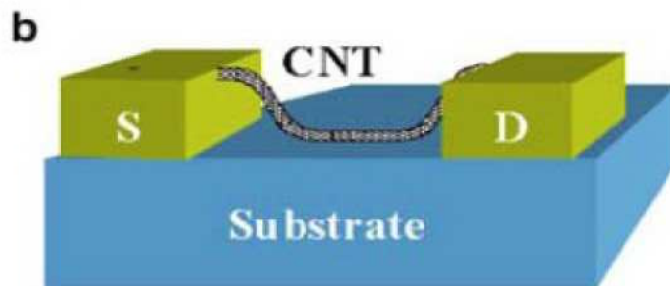


Temperature dependence of SbSI @ CNT d.c. resistance

($p = 10^{-3}$ mbar; vertical line represents $T_c = 293$ K for bulk crystals⁴¹)

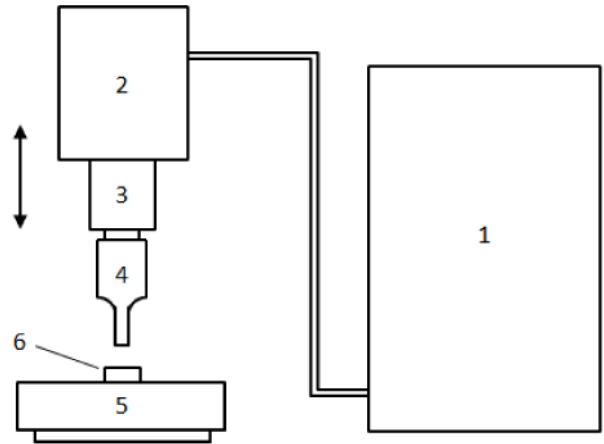


Al_2O_3 single crystal



Ultrasonic nanowelding

- 1 - ultrasonic generator 70 kHz
ADG70-100P-230-NO
(Rinco Ultrasonics)
- 3 - transducer C 70-2
(Rinco Ultrasonics)
- 5 - digital scale

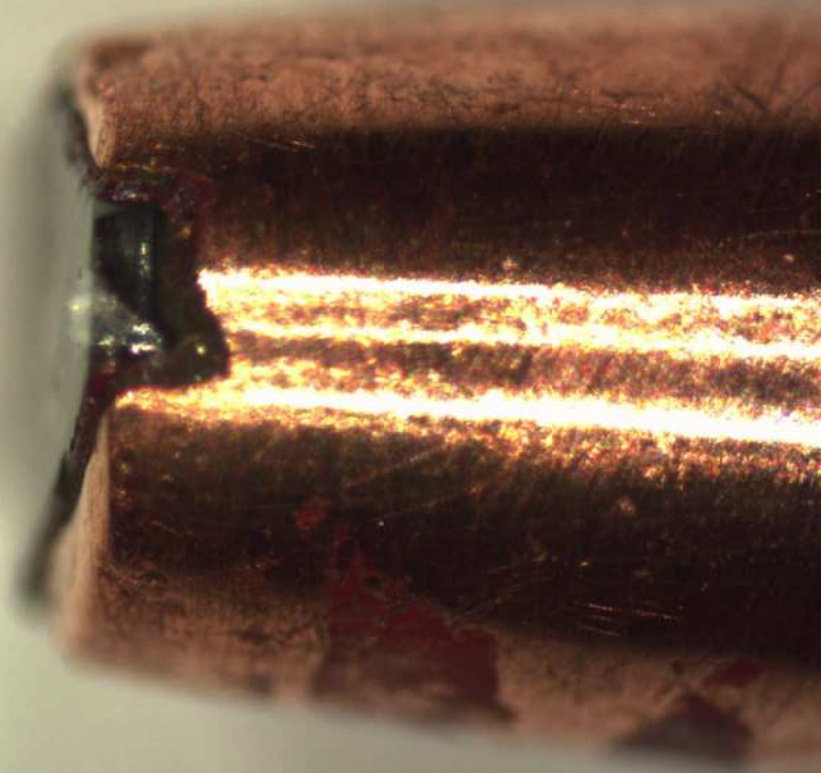


- 2 - holder
- 4 - special sonotrode made by myself
(surface roughness - order of
magnitude nm)
- 6 - sample



SiC single crystal

0.5 mm

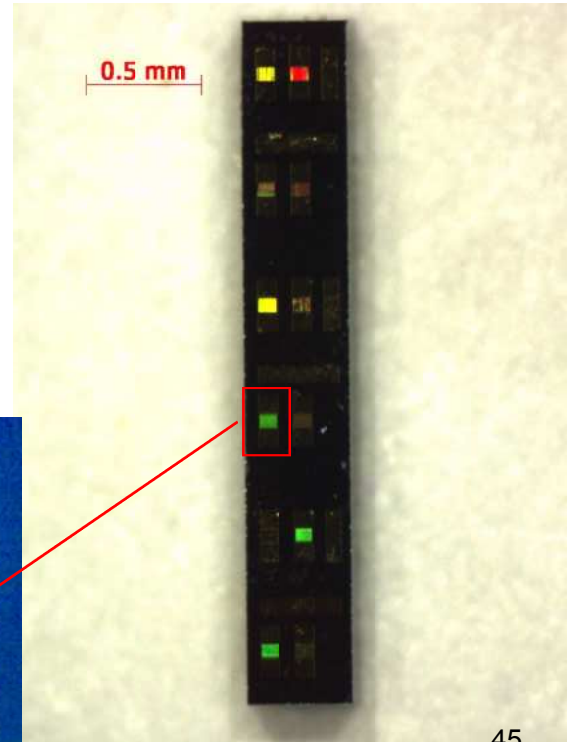
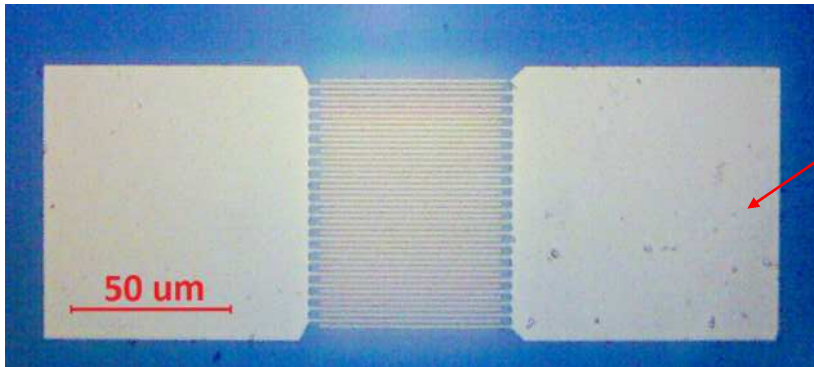
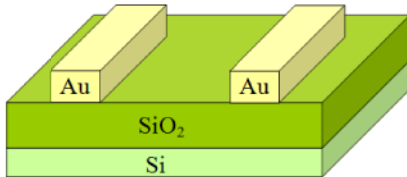


Si/SiO₂ substrates

made by:

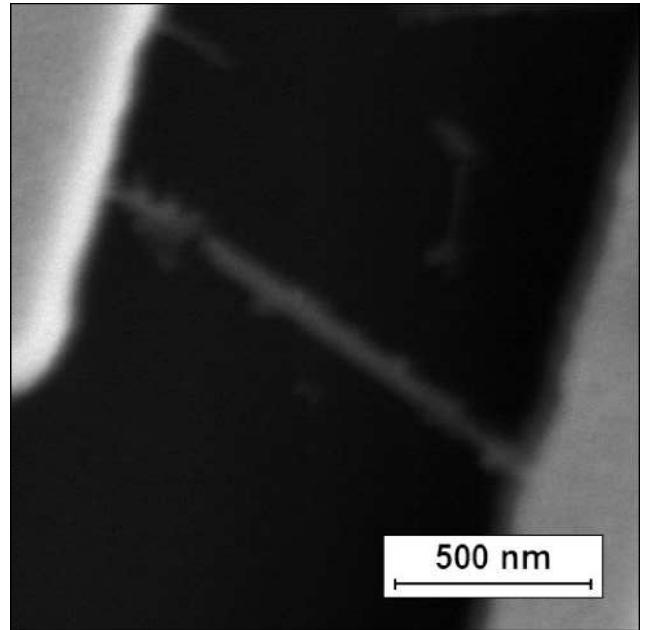
Wroclaw University of Technology;

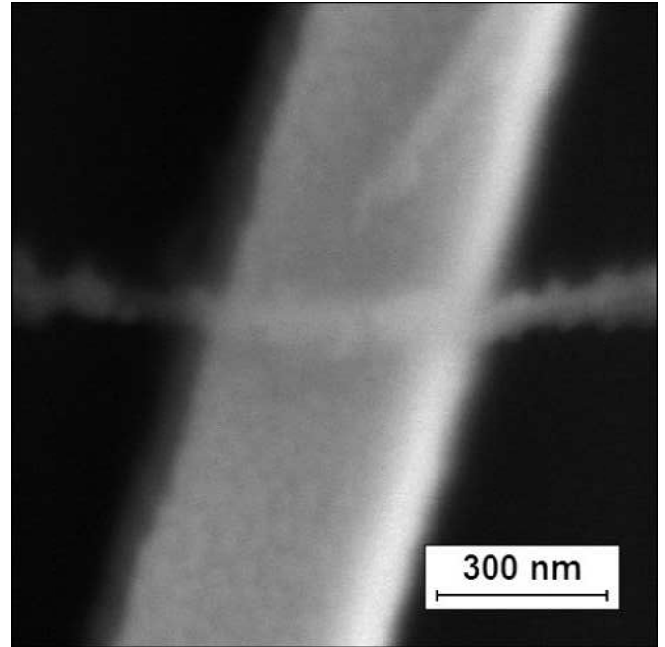
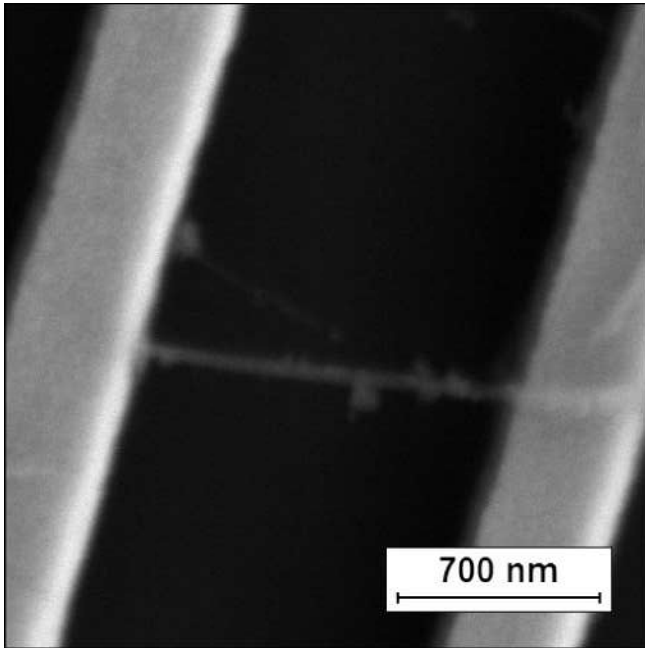
electrode spacing: 0.6, 1.2 or 2.5 μm



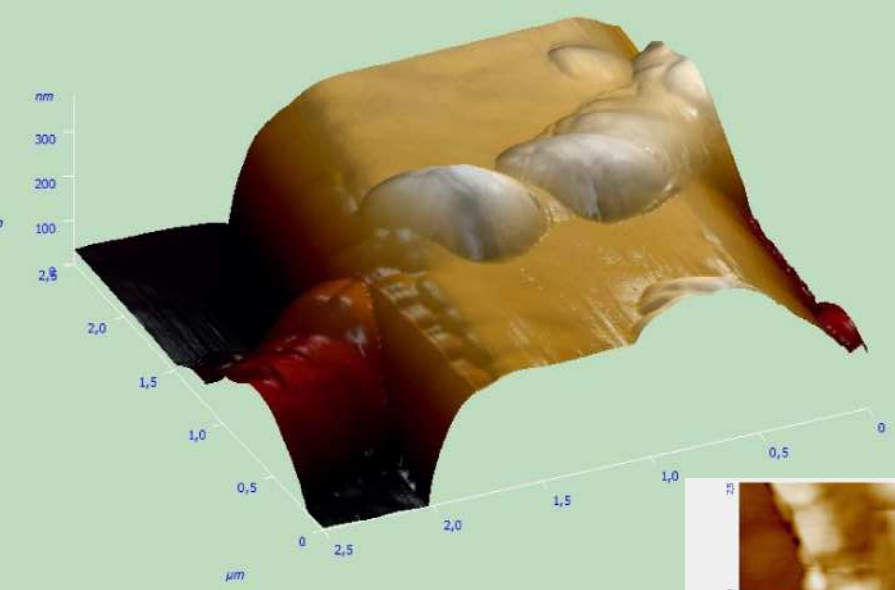
Alignment in electric field

- SbSI nanowires ultrasonically agitated in toluene ($\text{C}_6\text{H}_5\text{CH}_3$)
- applied electric field $E = \quad \cdot \quad ^5 \text{ V/m}$

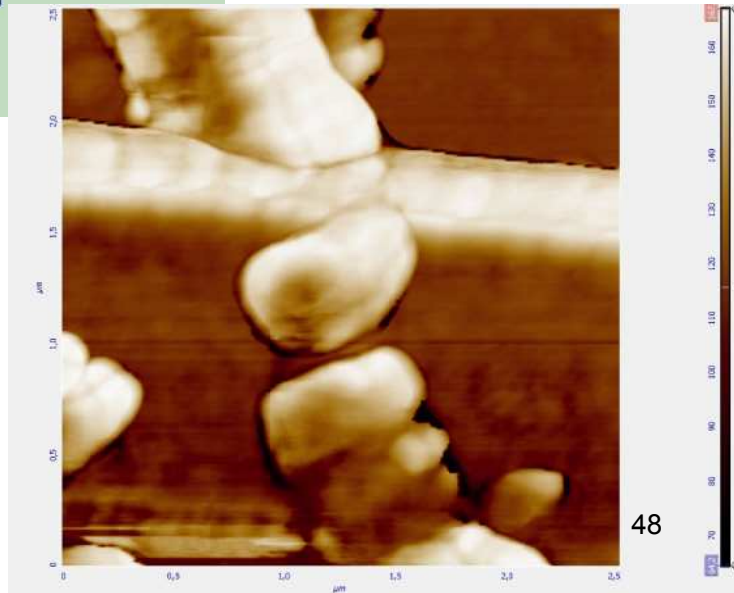




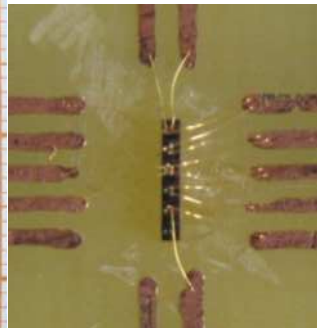
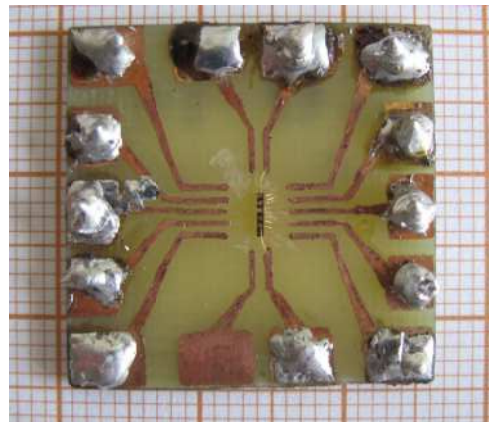
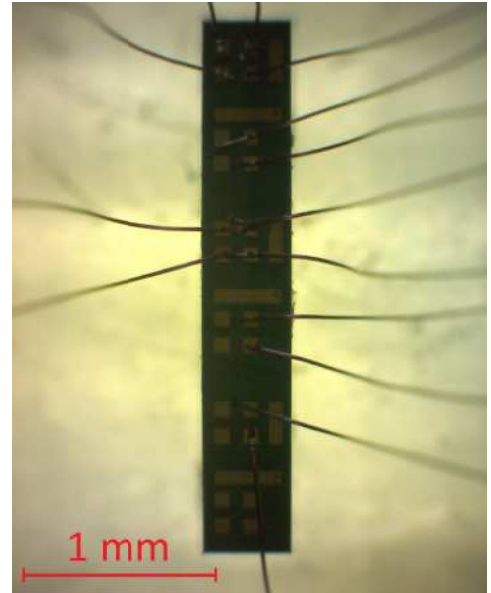
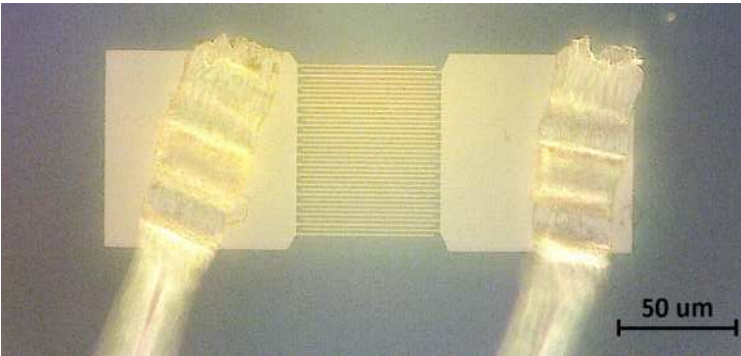
**SbSI nanowires on Si/SiO₂ substrate
with Au electrodes after ultrasonic nanowelding.**



**Nanowires of SbSI on
Si/SiO₂ substrate with Au
electrodes after
ultrasonic welding**

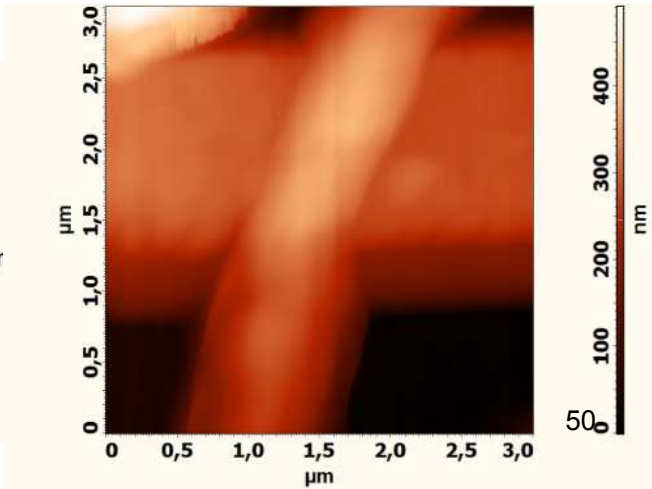
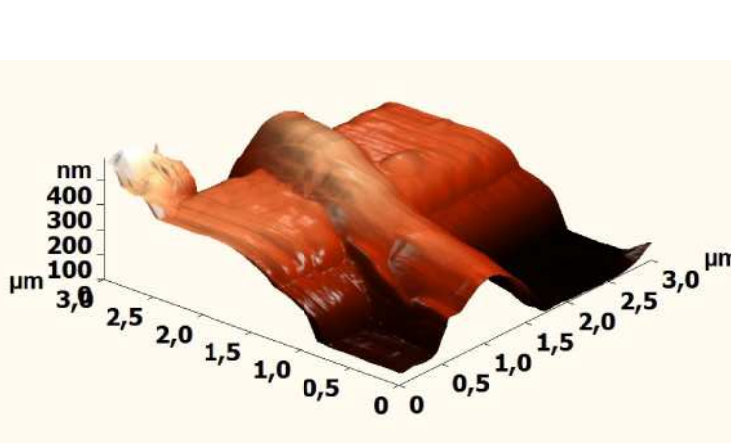
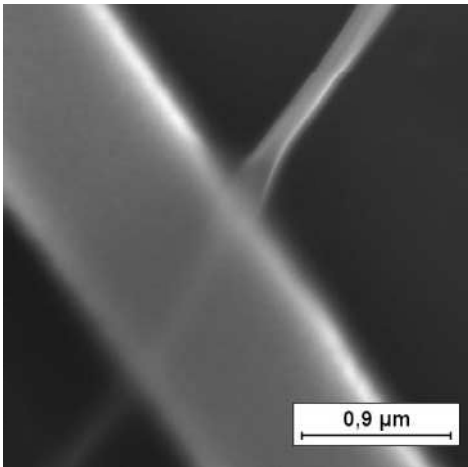
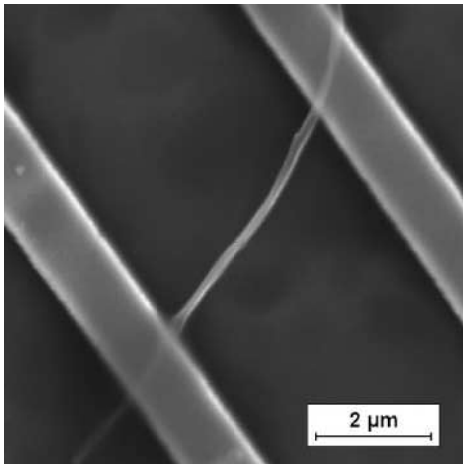
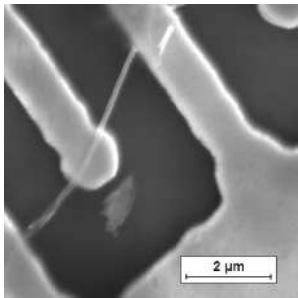


Ultrasonic bonding



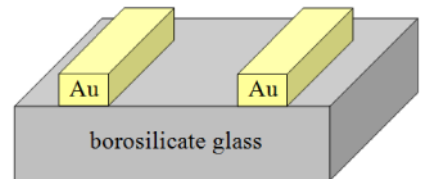
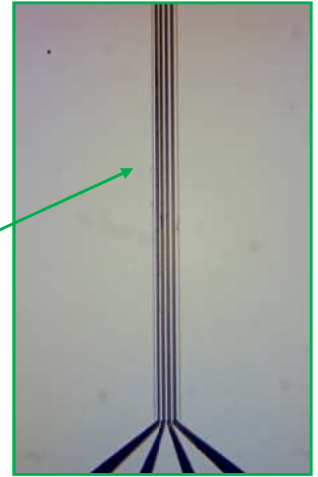
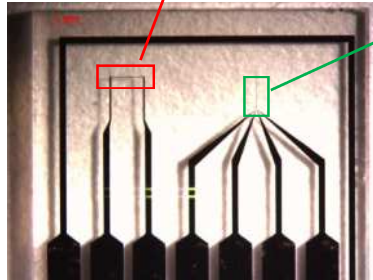
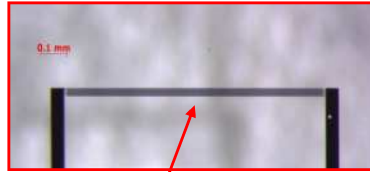
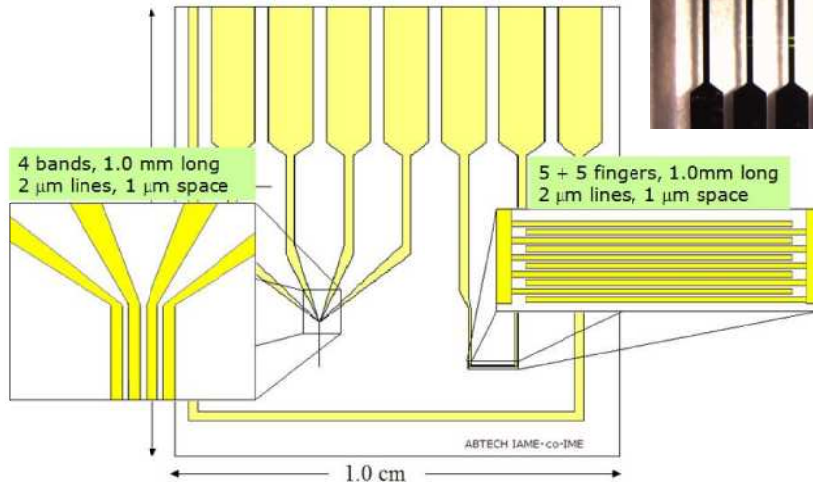
The electrical contacts made using wedge ultrasonic bonding.

Carbon nanotubes on Si/SiO₂ substrate with Au electrodes after ultrasonic welding

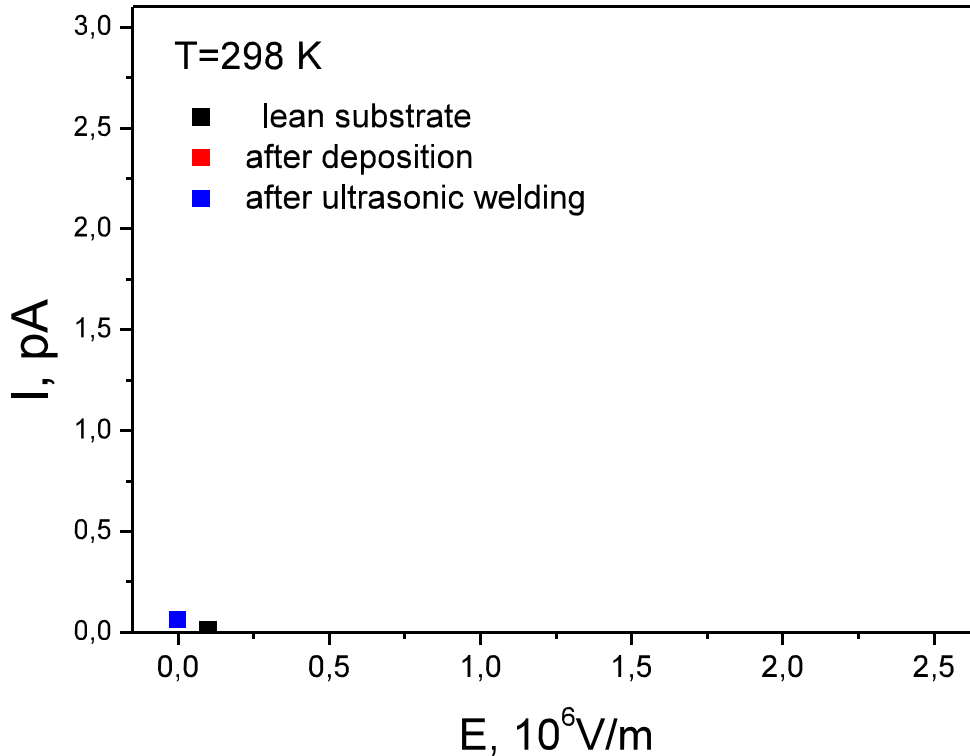


Glass Substrates

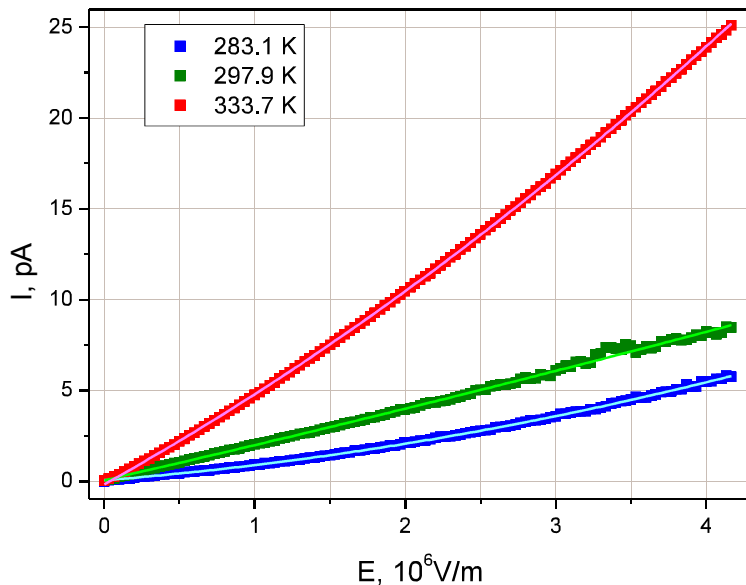
made by:
Abtech Scientific Inc.
electrode spacing: $1\ \mu\text{m}$



Nanowires of SbSI on glass substrate



DC electrical measurements



$$I = (A_0 E + B_0) + C_0 E^2 \quad [14]$$

ohmic conductivity space charge

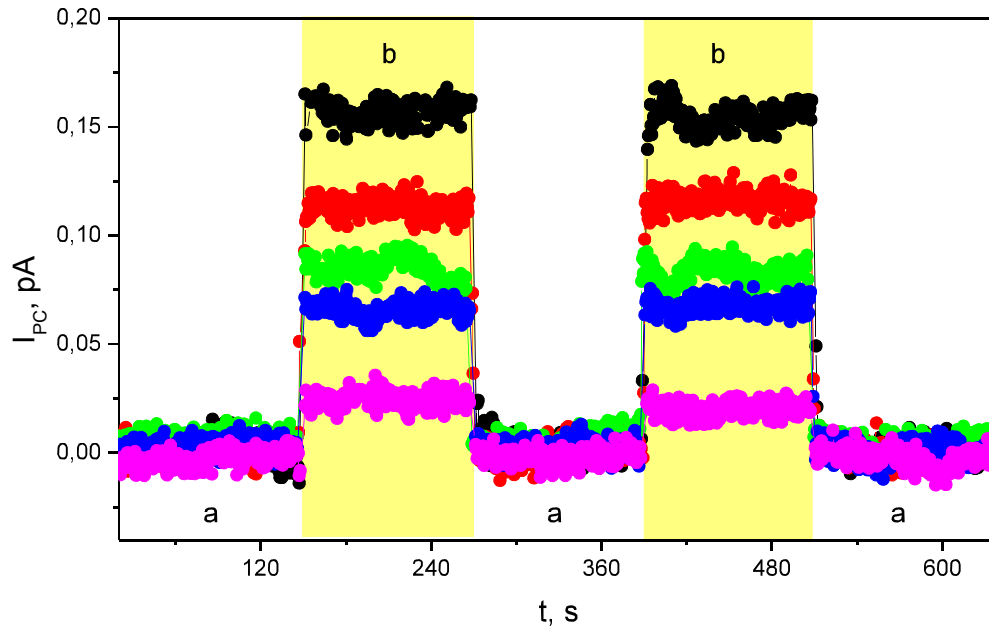
T, K	283.1	297.9	333.7
$A_0, 10^{-18} \text{ S}\cdot\text{m}$	0.662(10)	1.901(37)	4.607(14)
$B_0, 10^{-14} \text{ A}$	5.20(91)	5.0(33)	-17.9(13)
$C_0, 10^{-25} \text{ S}\cdot\text{m}^2/\text{V}$	1.717(23)	0.365(85)	3.574(33)

Current-voltage characteristics of SbSI single nanowires at different temperatures:

■ - $T=283.1 \text{ K}$; ■ - $T=297.9 \text{ K}$; ■ - $T=333.7 \text{ K}$; $p=1.3(7)\times 10^{-5} \text{ mbar}$;

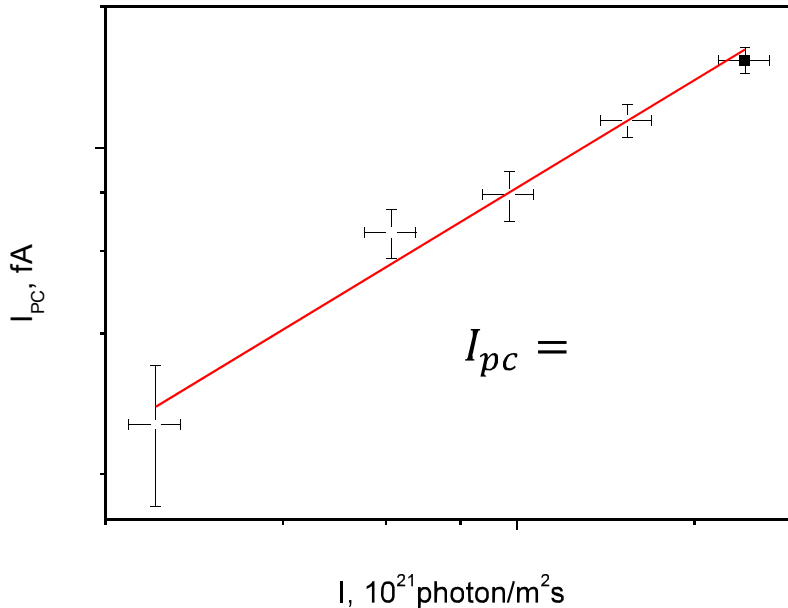
—, —, — fitted curves.

Photoconductivity of SbSI nanowires



Kinetics of photocurrent in unilluminated (a) and illuminated (b) SbSI nanowire measured for different light intensities: ■ - 100% I_0 , ■ - 63% I_0 , ■ - 40% I_0 , ■ - 25% I_0 , ■ - 10% I_0 ($\lambda=488$ nm, $I_0=2.4 \times 10^{22}$ photon/(m²s), $E=2.0 \times 10^6$ V/m, $T=298$ K).

Photoconductivity of SbSI nanowires



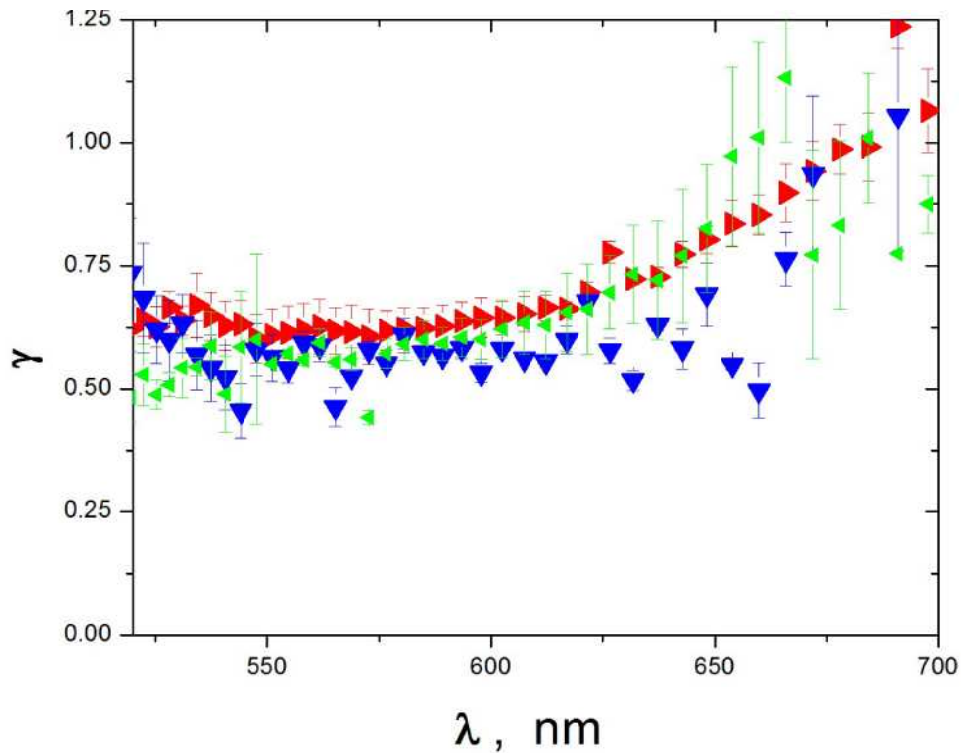
$$\gamma =$$

$$\cdot 10^{-30} \text{ A}$$

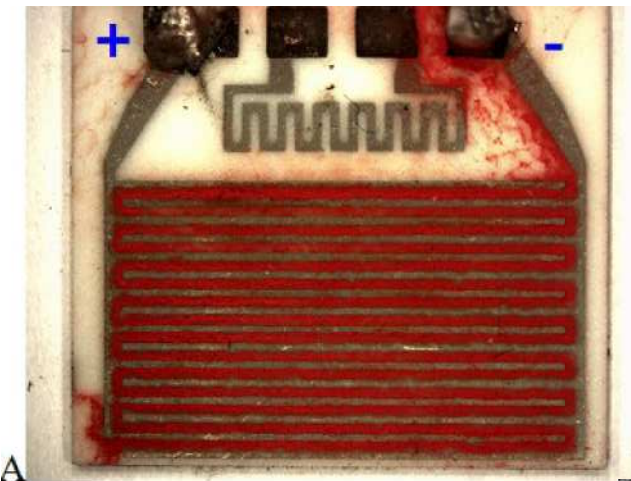
when: I_0 in photon/(m^2s)

Photocurrent as a function of light intensity
($\lambda=488 \text{ nm}$, $E=2.0 \times 10^6 \text{ V/m}$, $T=298 \text{ K}$).

$$I_{pc}(\lambda, T) = A(\lambda, T) I_0 \gamma(\lambda, T)$$

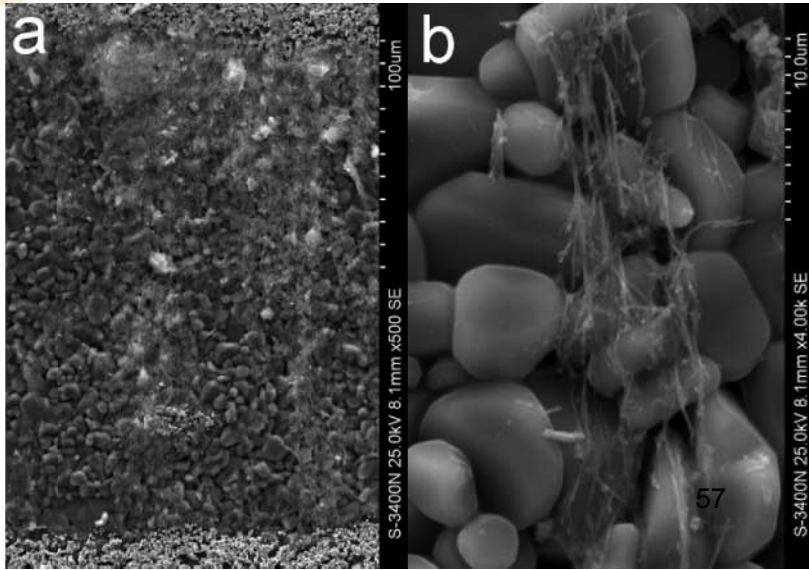


▼ - 283 K, ◀ - 303 K, ▶ - 323 K

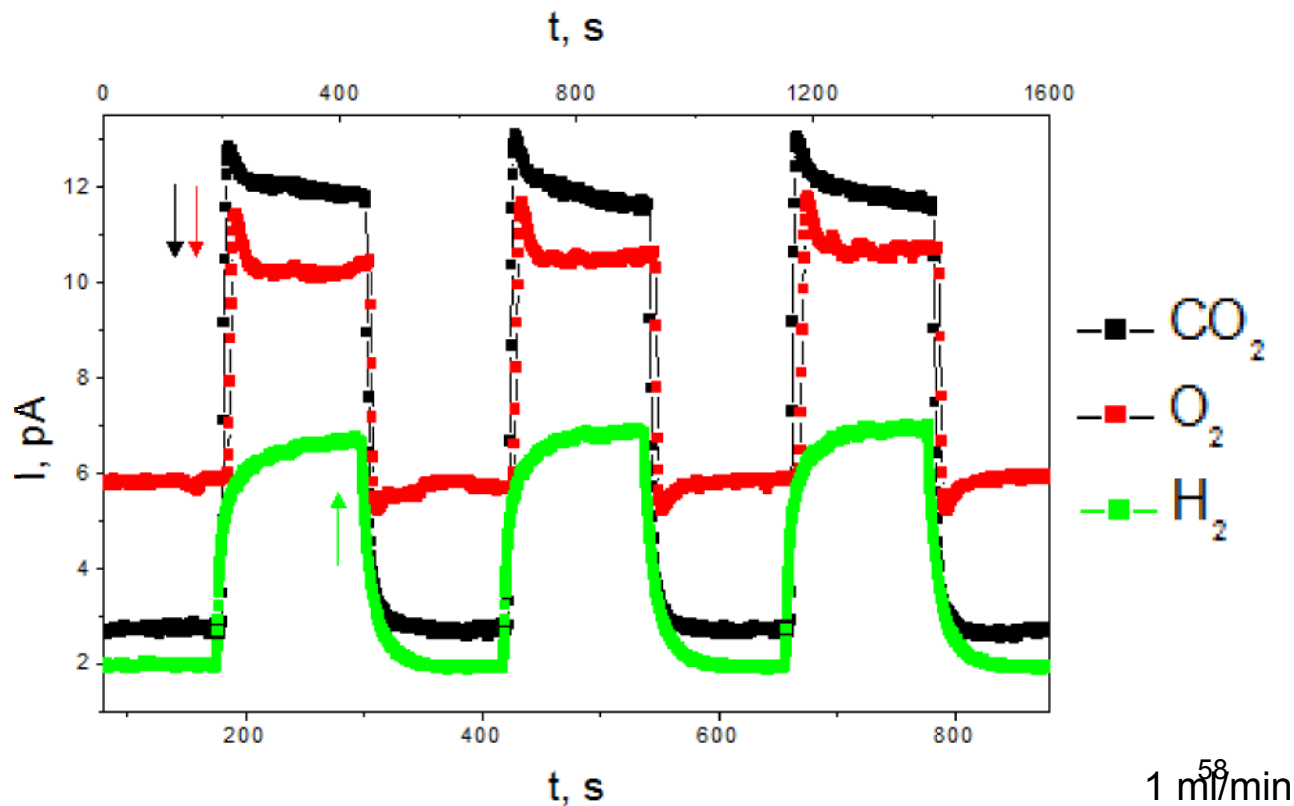


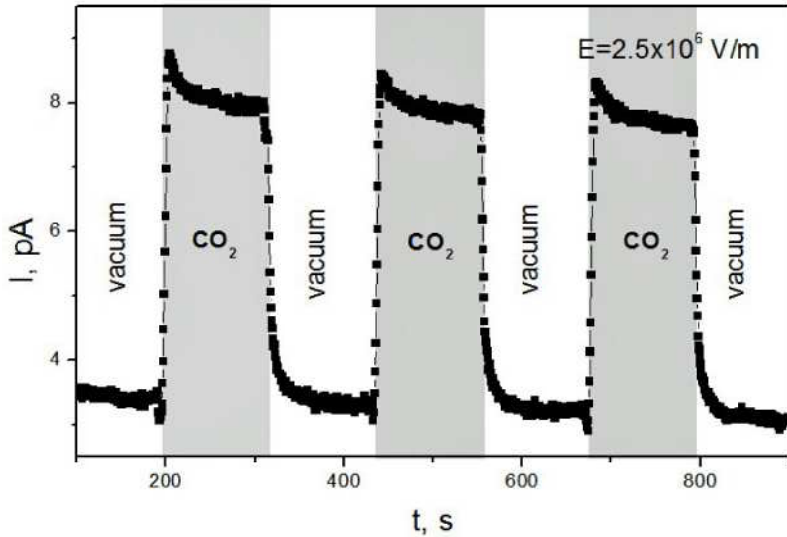
A 5 μm thick film of aligned SbSI nanowires on alumina substrate with interdigitated platinum lines as electrodes and the platinum temperature detector ($\cdot 5 \text{ V/m}$)

Low density of aligned SbSI nanowires on Al_2O_3 substrate ($\cdot 5 \text{ V/m}$)



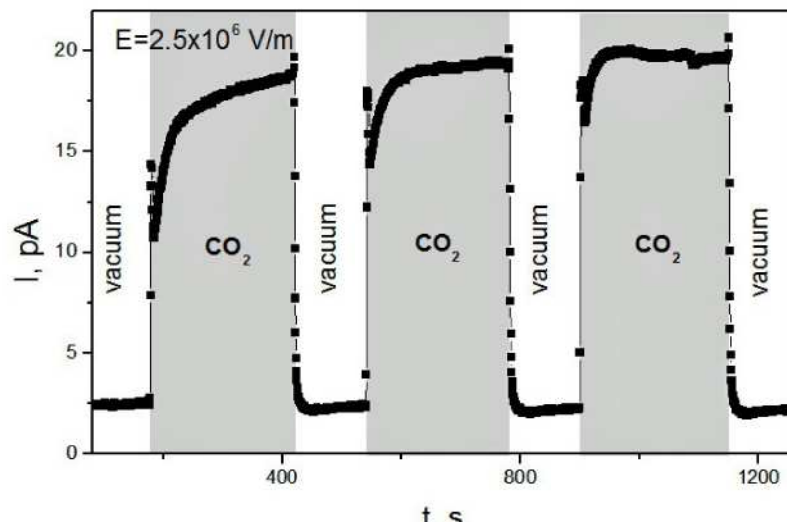
Nanowires of SbSI nanowelded to electrodes on glass substrate



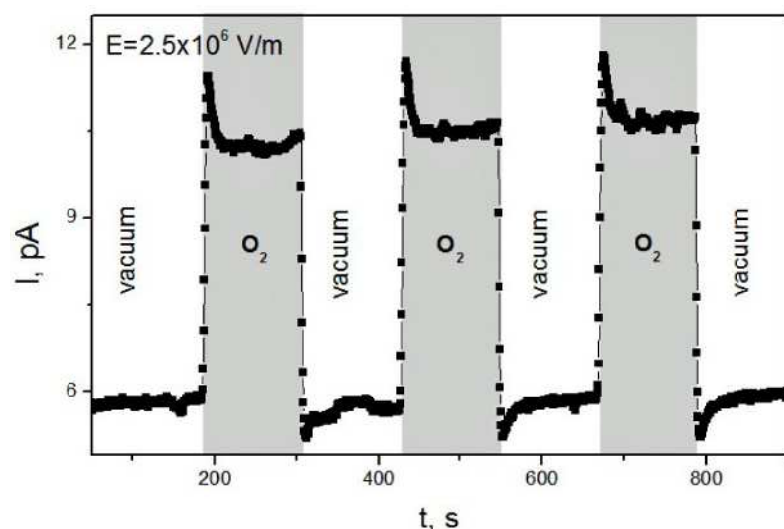


**SbSI nanowires nanowelded
to electrodes on glass
substrate**

0.5 ml/min

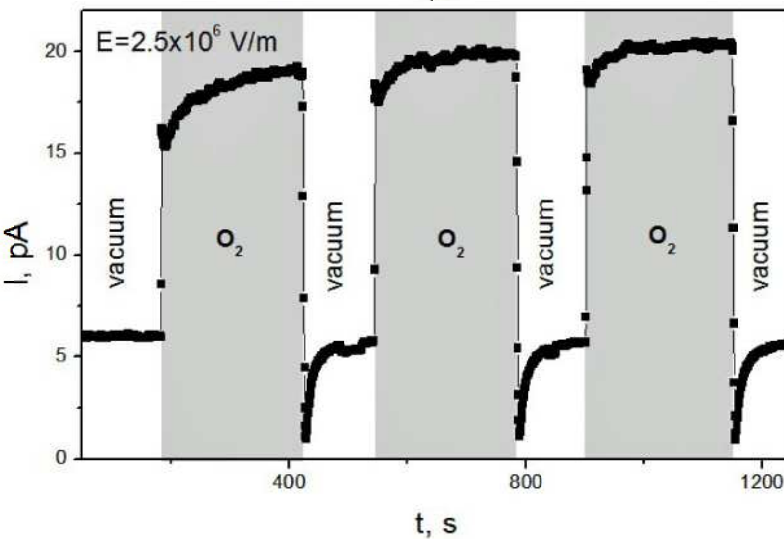


4 ml/min



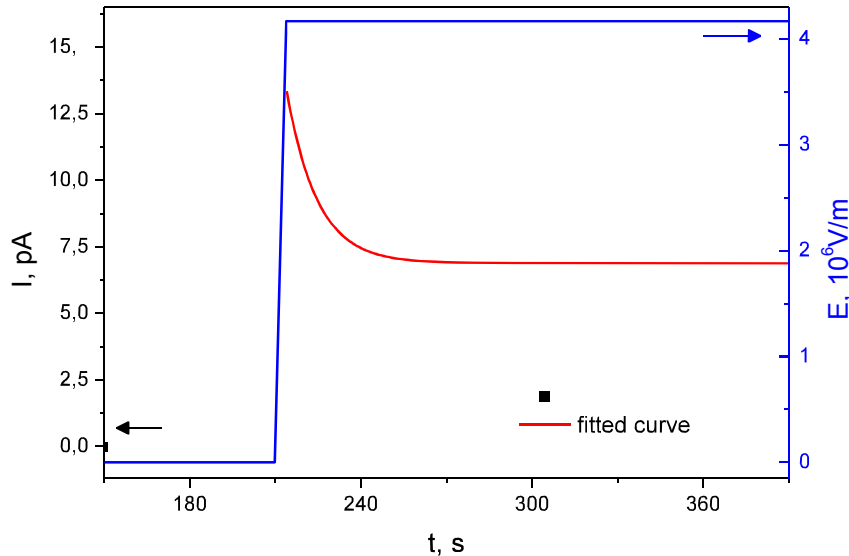
SbSI nanowires nanowelded to electrodes on glass substrate

1 ml/min



5 ml/min

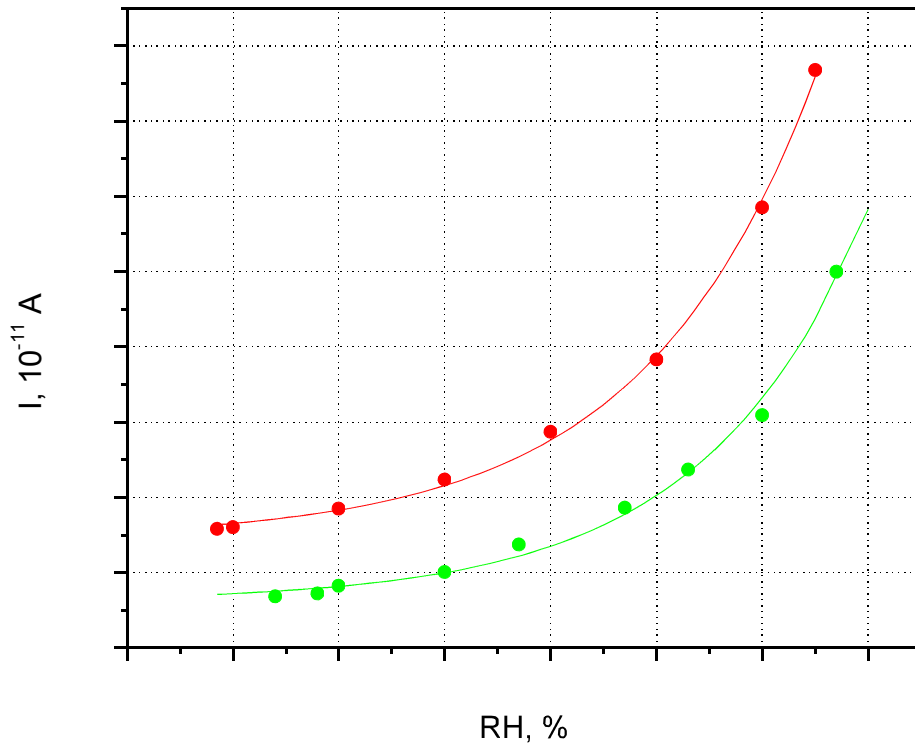
DC electrical measurements



$$I(t) = I_0 e^{-\frac{t}{\tau}} + I_{dc}$$

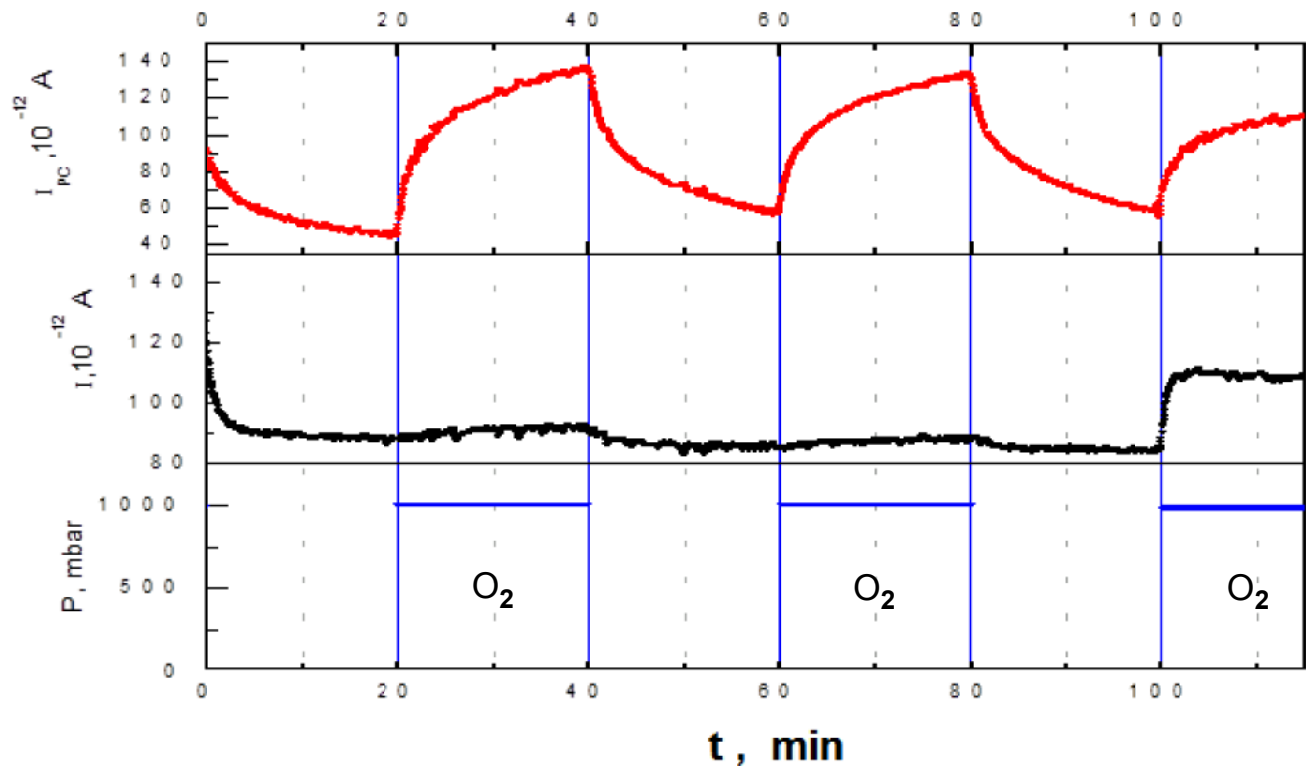
τ , s	10.74(28)
I_0 , mA	2.9(15)
I_{dc} , pA	6.879(16)

Time dependence of applied electric field (E) and current response (I) measured for SbSI single nanowires ($p=1.2 \times 10^{-5}$ mbar, $T=298.4$ K).

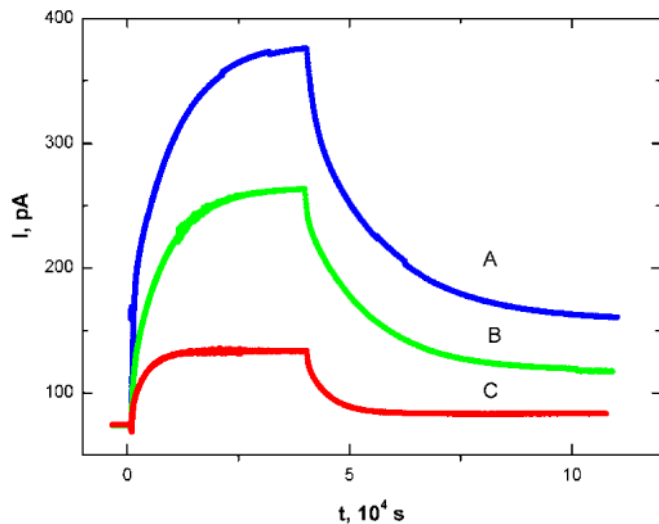


Current vs. relative humidity in the case of aligned non welded SbSI nanowires

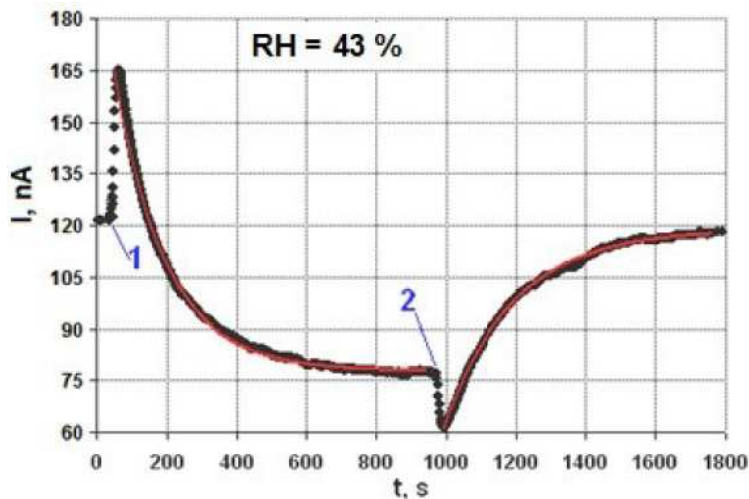
($\lambda=465$ nm; $I_0= \quad \cdot 10^{19}$ photon/(m²s); ● T = 280 K; ● T = 303 K)



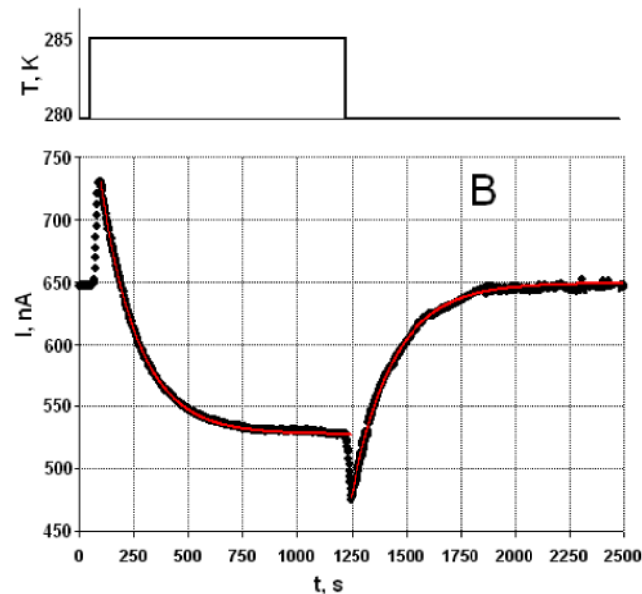
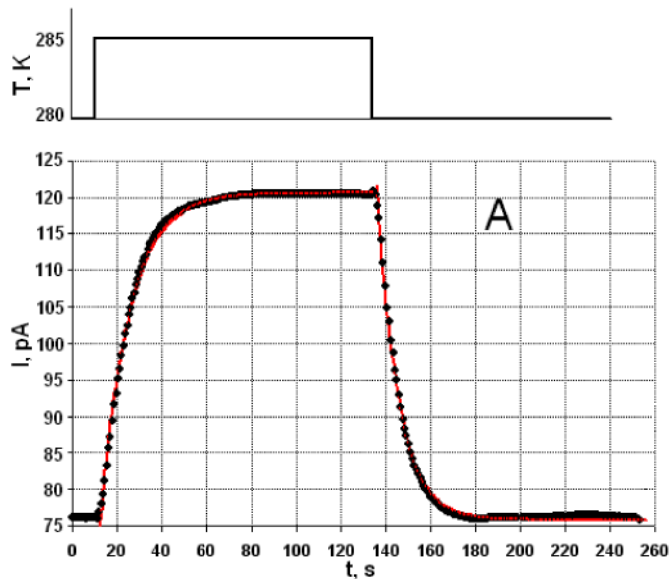
Kinetics of photocurrent in aligned non welded SbSI nanowires
 ($\lambda=465$ nm; $I_0 = 10^{19}$ photon/(m²s); T=303 K)



Kinetics of photocurrent in no welded SbSI xerogel in vacuum
 (A- $\lambda=465$ nm; B- $\lambda=518$ nm;
 C= $\lambda=660$ nm; $p=1.1$ mbar; $T=288$ K;
 $I_0 = \cdot 19$ photon/(m^2s))



Influence of humidity on kinetics of photocurrent in SbSI xerogel in N_2
 ($\lambda=488$ nm; $I_0 = \cdot 21$ photon/(m^2s))



Influence of temperature on electric current in SbSI xerogel in different environment

A- vacuum, $p=1.1$ mbar;

B- moist N₂ , RH=78 % at T=285 K and $p=987$ mbar.

Directions of future investigations

- gas nanosensors constructed from single nanowires of SbSI and SbSI@CNTs
- photodetectors constructed from single nanowires of SbSI and SbSI@CNTs

Authors are grateful to the Colaborators:

**dr. Piotr Szperlich
dr Mirosława Kępińska
dr Anna Starczewska
dr. Andrzej Nowrot
d .**

Institute of Physics, Silesian University of Technology, Katowice, Poland

**prof. Janusz Szala,
pro .
dr. Tomasz Rzychoń,
dr. Grzegorz Moskal
dr. Iwona Bednarczyk**

Department of Materials Science, Silesian University of Technology, Katowice, Poland

prof. Danuta Stróż,
Institute of Materials Science, University of Silesia, Katowice, Poland

**prof. Ewa Talik,
prof. Roman Wrzalik**
Institute of Physics, University of Silesia, Katowice, Poland

Thank you for your attention